

# The Role of Sterile Neutrinos in Cosmology and Astrophysics

Alexey Boyarsky<sup>\*†</sup>, Oleg Ruchayskiy<sup>‡</sup> and Mikhail Shaposhnikov<sup>‡</sup>

## Abstract

We present a comprehensive overview of an extension of the Standard Model that contains three right-handed (sterile) neutrinos with masses below the electroweak scale [the *Neutrino Minimal Standard Model*, ( $\nu$ MSM)]. We consider the history of the Universe from the inflationary era through today and demonstrate that most of the observed phenomena *beyond the Standard Model* can be explained within the framework of this model. We review the mechanism of baryon asymmetry of the Universe in the  $\nu$ MSM and discuss a dark matter candidate that can be warm or cold and satisfies all existing constraints. From the viewpoint of particle physics the model provides an explanation for neutrino flavor oscillations. Verification of the  $\nu$ MSM is possible with existing experimental techniques.

## Keywords:

$\nu$ MSM; neutrino oscillations; baryogenesis; dark matter; inflation

## 1 Introduction

The Standard Model (SM) of elementary particles [1, 2, 3], defined as a renormalizable field theory, based on the  $SU(3) \times SU(2) \times U(1)$  gauge group, and containing three fermionic families — left-handed particles,  $SU(2)$  doublets, right-handed particles,  $SU(2)$  singlets (no right-handed neutrinos) and one Higgs doublet — has successfully predicted a number of particles and their properties. However, there is no doubt that the SM is not a final theory. Indeed, over the past several decades it

---

<sup>\*</sup>Institute of Theoretical Physics, ETH Hönggerberg, CH-8093 Zürich, Switzerland

<sup>†</sup>Bogolyubov Institute for Theoretical Physics, Kiev 03680, Ukraine

<sup>‡</sup>Institute of Theoretical Physics École Polytechnique Fédérale de Lausanne, FSB/ITP/LPPC, BSP, CH-1015, Lausanne, Switzerland

has become increasingly clear that it fails to explain a number of *observed* phenomena in particle physics, astrophysics, and cosmology. These phenomena *beyond the SM* (BSM) are (a) neutrino oscillations (transition between neutrinos of different flavors), (b) baryon asymmetry (excess of matter over anti-matter in the Universe), (c) dark matter (about 80% of all matter in the Universe consisting of unknown particles), (d) inflation (a period of rapid accelerated expansion in the early Universe), and (e) dark energy (late-time accelerated expansion of the Universe) This list of *well-established observational* drawbacks of the SM is considered complete at present. All the other BSM problems — for, instance, the gauge hierarchy and strong-CP problems — require theoretical fine-tuning.

At what energies should the SM be superseded by some other, more fundamental theory? The existence of gravity with the coupling related to the Planck scale —  $M_{Pl} = G_N^{-1/2} = 1.2 \times 10^{19}$  GeV, where  $G_N$  is the Newtonian gravitational constant — implies that the cut-off is *at least* below the Planck scale. If the cutoff is identified with  $M_{Pl}$ , the low-energy Lagrangian can contain all sorts of higher-dimensional  $SU(3) \times SU(2) \times U(1)$ -invariant operators that are suppressed by the Planck scale,

$$\mathcal{L} = \mathcal{L}_{SM} + \sum_{n=5}^{\infty} \frac{\mathcal{O}_n}{M_{Pl}^{n-4}}, \quad (1)$$

where  $\mathcal{L}_{SM}$  is the Lagrangian of the SM. These operators lead to a number of physical effects that cannot be described by the SM, such as neutrino masses and mixings, proton decay, etc. However, as we will discuss below, even the theory shown in Eq. (1) does not survive when confronted with different experiments and observations.

Alternatively, one can place a cut-off  $\Lambda \ll M_{Pl}$  in Eq. (1), which would imply that new physics (and new particles) appears well below the Planck scale at energies  $E \sim \Lambda$ . If  $\Lambda \gg M_W$ , where  $M_W$  is the mass of the weak  $W$  boson, the resulting theory suffers from the so-called *gauge hierarchy problem*, that is, the problem of quantum stability of the mass of the Higgs boson against quantum corrections from heavy particles.

Most of the research in BSM physics carried out during the past few decades was devoted to solving the gauge hierarchy problem. Many different suggestions were proposed concerning how to achieve the “naturalness” of electroweak symmetry breaking. These propositions are based on supersymmetry, technicolor, and large extra dimensions, among other ideas. Finding a solution to the gauge hierarchy problem, coupled with the need to solve observational and other fine-tuning problems of the SM, is extremely challenging. Most of the approaches postulate the existence of new particles with masses *above* the electroweak scale (ranging from  $10^2$  GeV to  $10^{15}$ – $10^{16}$  GeV). As a result, the proposed theories contain a plethora of (not yet observed) new particles and parameters.

In this review, we describe a conceptually different scenario for BSM physics and its consequences for astrophysics and cosmology in an attempt to address the BSM problems named above *without* introducing new energy scales (that is, in addition to the electroweak and the Planck scales). In such an approach, the hierarchy problem is shifted to the Planck scale, and there is no reason to believe that the field theoretical logic is still applicable to it.

Below we show (following Refs. [4, 5] and a number of subsequent works) that this goal may be achieved with a very simple extension of the SM. The only new particles, added to the SM Lagrangian are three gauge-singlet fermions (i.e., *sterile neutrinos*) with masses *below* the electroweak scale. Right-handed neutrinos are strongly motivated by the observation of neutrino flavor oscillations. In Section 2 we review neutrino oscillations and introduce the corresponding Lagrangian. We summarize the choice of parameters of the Neutrino Minimal Standard Model ( $\nu$ MSM) in Section 3. In Section 4, we present a  $\nu$ MSM cosmology. We discuss the restrictions from astrophysics, cosmology, and particle physics experiments, as well as future searches in Section 5. In Section 6, we conclude with a discussion of possible extensions of the  $\nu$ MSM and potential astrophysical applications of sterile neutrinos.

## 2 Neutrino oscillations

When the SM was conceived, neutrinos were thought to be massless and different lepton numbers were believed to be conserved (which would not be the case if right-handed neutrinos were present). This was a reason for *not introducing right-handed neutrinos* decades ago.

Transitions between neutrinos of different flavors have been observed. These *neutrino oscillations* manifest themselves in experiments with solar, atmospheric, accelerator and reactor neutrinos. The subject of neutrino oscillations has received a great deal of attention in recent years and many reviews are available (see e.g. Refs. [6, 7]). The observed oscillations determine the mass differences between propagation states [8]

$$\Delta m_{\text{sun}}^2 = 7.65_{-0.20}^{+0.23} \times 10^{-5} \text{ eV}^2 \quad (2)$$

and

$$|\Delta m_{\text{atm}}^2| = 2.40_{-0.11}^{+0.12} \times 10^{-3} \text{ eV}^2. \quad (3)$$

Importantly, each of these results was confirmed by two different types of experiments: accelerator [9] for Eq. (3) and reactor [10] for Eq. (2).

The observed pattern of neutrino oscillations cannot be explained by the action Eq. (1) with the Planck-scale cutoff. Indeed, the lowest-order five-dimensional

operator

$$\mathcal{O}_5 = A_{\alpha\beta} \left( \bar{L}_\alpha \tilde{\phi} \right) (\phi^\dagger L_\beta^c) \quad (4)$$

leads to the Majorana neutrino masses of the order  $m_\nu \sim v^2/M_{Pl} \simeq 10^{-6}$  eV, where  $L_\alpha$  are left-handed leptonic doublets, the index  $\alpha = e, \mu, \tau$  labels generations,  $\phi$  is a Higgs doublet with  $\tilde{\phi}_j = i(\tau_2)_j^k \phi_k^*$ ,  $c$  is the sign of charge conjugation, and  $v = 174$  GeV is the vacuum expectation value of the Higgs field.

The fact that the  $m_\nu$  following from this Lagrangian is so small compared with the lower bound on neutrino mass arising from the observations of neutrino oscillations ( $m_\nu > \sqrt{|\Delta m_{\text{atm}}^2|} \simeq 0.05$  eV) rules out the conjecture that the theory shown in Eq. (1) is a viable effective field theory up to the Planck scale. Therefore, *the existence of neutrino oscillations requires adding new particles to the Lagrangian of the Standard Model.*

Let us add  $\mathcal{N}$  right-handed neutrinos  $N_I$  ( $I = 1, \mathcal{N}$ ). The most general renormalizable Lagrangian has the form:

$$\mathcal{L} = \mathcal{L}_{SM} + i\bar{N}_I \partial_\mu \gamma^\mu N_I - \left( F_{\alpha I} \bar{L}_\alpha N_I \tilde{\phi} - \frac{M_I}{2} \bar{N}_I^c N_I + h.c. \right), \quad (5)$$

where  $F_{\alpha I}$  are new Yukawa couplings. The right-handed neutrinos have zero electric, weak and strong charges; therefore, they are often termed “singlet,” or “sterile” fermions. The Majorana masses  $M_I$  are consistent with the gauge symmetries of the SM. Without loss of generality, the Majorana mass matrix in diagonal form can be chosen.

If the Dirac masses  $M_D = F_{\alpha I} \langle \phi \rangle$  are much smaller than the Majorana masses  $M_I$ , *the type I seesaw formula* [11, 12, 13, 14] holds that

$$(m_\nu)_{\alpha\beta} = - \sum_{I=1}^{\mathcal{N}} (M_D)_{\alpha I} \frac{1}{M_I} (M_D^T)_{I\beta}, \quad (6)$$

where  $m_\nu$  is a  $3 \times 3$  matrix of active neutrino masses, mixings, and (possible) CP-violating phases. An elementary analysis of Eq. (6) shows that the number of right-handed singlet fermions  $\mathcal{N}$  must be *at least two* to fit the data of neutrino oscillations. If there were only one sterile neutrino, then the two active neutrinos would be massless. If there were two singlet fermions, only one of the active neutrinos would be massless, which does not contradict the results from experiment. Moreover, in this case there are 11 new parameters in the Lagrangian (5) — two Majorana masses, two Dirac masses, four mixing angles, and three CP-violating phases — which is more than the number of parameters (7) describing the mass matrix of active neutrinos with one zero eigenvalue. In other words, for  $\mathcal{N} = 2$  the Lagrangian (5) can describe the pattern of neutrino masses and mixings observed experimentally. Of course, the situation is even more relaxed for  $\mathcal{N} = 3$ . The

Lagrangian (5) with  $\mathcal{N} = 3$  restores the symmetry between quarks and leptons: Every left quark and lepton has a right counterpart.

The seesaw formula (6) allows the mass of singlet neutrinos to be a free parameter: Multiplying  $M_D$  by any number  $x$  and  $M_I$  by  $x^2$  does not change the right-hand side of the formula. Therefore, the choice of  $M_I$  is a matter of theoretical prejudice that cannot be fixed by active-neutrino experiments alone.

In this review, our choice of  $M_I$  is roughly of the order of the other mass term in the Lagrangian of the SM, the mass of the Higgs boson. This choice does not lead to any intermediate scale between the electroweak and Planck scales, but it does require small Yukawa couplings  $F_{\alpha I}$ . It allows us to solve, in a unified manner, the observational problems of the SM discussed above. Specifically, the parameters of the model (5) can be chosen such that it provides a mechanism to generate baryon asymmetry of the Universe (BAU) and a dark matter candidate in the form of the lightest sterile neutrino. Also, this theory can accommodate inflation, if one considers non-minimal coupling between the Higgs boson and gravity [15]. Finally, a scale-invariant extension of the model [16, 17] that includes unimodular gravity may solve the problem of stability of the Higgs mass against radiative corrections, even if the Planck scale is included, and could lead to an explanation of dark energy and of the absence of the cosmological constant.

The Lagrangian (5) with such a choice of parameters, explaining all confirmed BSM phenomena,<sup>1</sup> has been termed the  $\nu$ MSM—the *Neutrino Minimal Standard Model* [5, 4].

### 3 A choice of parameters: the $\nu$ MSM

In this section we discuss in detail how the parameters of the Lagrangian (5) should be chosen so as to explain the BSM phenomena without introducing new physics above the electroweak scale.

#### 3.1 Neutrino masses and oscillations

As discussed above, the Lagrangian (5) can explain any pattern of active neutrino masses and mixings. A naturalness argument [23], reproduced below, indicates

---

<sup>1</sup>There are also several unexplained phenomena in astrophysics (e.g., the 0.511-MeV line from the Galactic center [18], pulsar-kick velocities [19], a feature in the positron spectrum at  $\sim 100$  GeV [20], etc.). We do not consider them in this review, as for these phenomena standard physics explanations may exist. Note, however, that the sterile neutrinos may play an important role in some of these cases (see Section 6). In addition, several anomalies in particle physics experiments (such as evidence for the neutrinoless double-beta decay [21] and the annual modulation of signal, observed by DAMA/LIBRA [22]) have been reported. However, none of them has yet been confirmed by other experiments.

that the masses  $M_I$  should be smaller than  $10^7$  GeV. Indeed, the stability of the Higgs mass against radiative corrections, which arise from  $N_I$ -exchange in the loops, requires

$$\frac{1}{16\pi^2} \sum_{\alpha I} |F_{\alpha I}|^2 M_I^2 \lesssim M_H^2, \quad (7)$$

where  $M_H$  is the Higgs mass. Combining this equation with the seesaw formula (6) leads to

$$M_I \lesssim \left( \frac{16\pi^2 M_H^2 v^2}{\sqrt{|\Delta m_{\text{atm}}^2|}} \right)^{\frac{1}{3}} \simeq 10^7 \text{ GeV}. \quad (8)$$

Any  $M_I$  mass below this value is “natural”. Also note that setting  $M_I$  to zero increases the symmetry of the Lagrangian (introducing lepton number conservation) and thus this choice is also stable against radiative corrections. In the  $\nu$ MSM approach, we set  $M_I$  below the electroweak scale, so that these new particles are on the same footing as known quarks and leptons.

The observed existence of two mass splittings (solar and atmospheric, Eqs. (2–3)) requires at least two sterile neutrinos. To estimate what neutrino data imply for the Yukawa couplings, we take the larger of the two mass splittings  $|\Delta m_{\text{atm}}^2|$  and find from the seesaw relations (6) that

$$|F|^2 \approx \frac{\sqrt{|\Delta m_{\text{atm}}^2|} M_I}{v^2} \sim 2 \times 10^{-15} \frac{M_I}{\text{GeV}}. \quad (9)$$

where  $|F|^2$  is a typical value of Yukawa couplings  $F_{\alpha I}$ . The condition  $M_I \lesssim 10^2$  GeV implies that  $|F|^2 \lesssim 10^{-13}$ . Clearly, the theory given in Eq. (5) can describe neutrino oscillation data even if one of the three sterile neutrinos has arbitrarily small Yukawa couplings.

Another possible choice of parameters of the Lagrangian (5), suffering from the hierarchy problem described in Reference [23], relates the smallness of the neutrino masses to the largeness of the Majorana mass terms  $M_I$ . Indeed, if we take the Yukawa couplings  $F_{\alpha I} \sim 1$  and the Majorana masses in the range  $M_I \sim 10^{10} - 10^{15}$  GeV, we obtain the neutrino masses, as required by experimental observations. An attractive feature of this scenario is that this new scale may be associated with the Grand Unification Theory (GUT) scale. A model (5) with this choice of parameters can also give rise to BAU through leptogenesis [24] and anomalous electroweak number non-conservation at high temperatures [25]. However, we do not discuss this possibility here; for review of the GUT-scale seesaw and the thermal leptogenesis scenario associated with it, see, for instance, Reference [26].<sup>2</sup>

---

<sup>2</sup>There is still another choice of seesaw parameters with a sterile neutrino mass  $\sim 1$  eV [27], which we do not discuss here.

### 3.2 Dark matter candidate

It has been noticed that a sterile neutrino may make an interesting dark matter candidate [28, 29, 30, 31, 32]. In the  $\nu$ MSM, a dark matter sterile neutrino is simply one of the singlet fermions (for definiteness, we consider it to be  $N_1$ ). The interaction strength between the sterile neutrino and the matter is *superweak* with the characteristic strength  $\theta G_F$ , where  $G_F$  is the Fermi constant and where the *mixing angle*  $\theta \ll 1$  is defined as

$$\theta_1^2 = \sum_{\alpha=e,\mu,\tau} \frac{v^2 |F_{\alpha 1}|^2}{M_1^2}. \quad (10)$$

Based on the universal Tremaine–Gunn bound [33], the masses of sterile neutrinos are restricted to the keV range and above. Specifically, for fermionic DM particles an *average* phase-space density in any dark matter-dominated system cannot exceed the density given by the Pauli exclusion principle. Applied to the smallest dark matter-dominated objects [dwarf spheroidal galaxies of the Milky Way, (dSphs)] this bound translates into  $M_{\text{DM}} \geq 400$  eV [34].

A sterile neutrino is an example of *decaying* DM. Through its mixing with the ordinary neutrinos,  $N_1$  can decay (via  $Z$  boson exchange) into three (anti)neutrinos. To be DM, the lifetime of  $N_1$  should be greater than the age of the Universe, which restricts the mixing angle. A significantly stronger constraint comes from a subdominant one-loop decay channel into a photon and an active neutrino. The energy of the produced photon is  $E_\gamma = M_1/2$ , and the decay width is given by [35, 36]

$$\Gamma_{N_1 \rightarrow \gamma \nu} = \frac{9 \alpha G_F^2}{1024 \pi^4} \sin^2(2\theta_1) M_1^5 \simeq 5.5 \times 10^{-22} \theta_1^2 \left[ \frac{M_1}{\text{keV}} \right]^5 \text{ s}^{-1}, \quad (11)$$

where  $\alpha$  is the fine-structure constant. The expression for the width of the dominant decay channel has the same parametric form, with the numeric coefficient being  $\sim 128$  times larger. This radiative decay would produce a narrow line, for instance, in the diffuse X/ $\gamma$ -ray background [30, 32]. This gives a restriction on the mixing angle,

$$\theta_1^2 \lesssim 1.8 \times 10^{-5} \left( \frac{\text{keV}}{M_1} \right)^5, \quad (12)$$

meaning that the lifetime of sterile neutrino DM  $\tau_{N_1 \rightarrow 3\nu}$  exceeds  $10^{24}$  sec [37] — six orders of magnitude longer than the age of the Universe. We discuss X-ray constraints in detail in Section 5.1.

The contribution of the  $N_1$  sterile neutrino to the masses of the active neutrinos is of the order  $\delta m_\nu \sim \theta_1^2 M_1$ . The lifetime constraints mean that for  $M_1 \gtrsim 2$  keV the correction  $\delta m_\nu$  is less than the error bar in the solar neutrino mass difference (2).

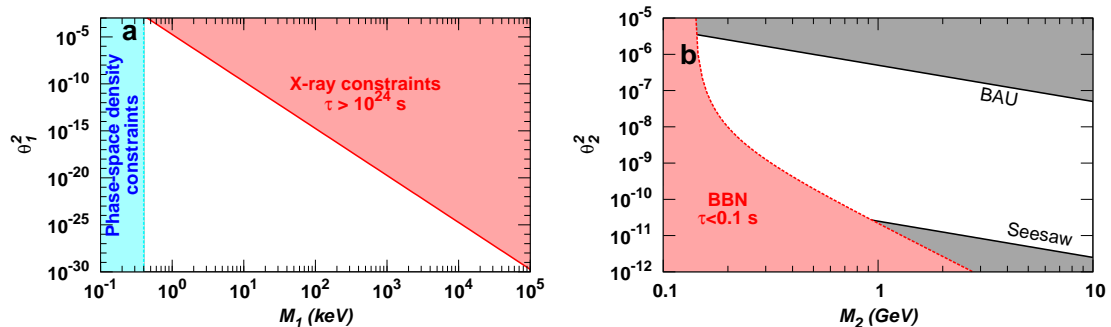


Figure 1: Constraints on the masses and mixing angles of the dark matter sterile neutrino  $N_1$  (a) and of two heavier sterile neutrinos  $N_{2,3}$  (b). These constraints come from astrophysics, cosmology, and neutrino oscillation experiments. Abbreviations: BAU, baryon asymmetry of the Universe; BBN, big bang nucleosynthesis.

This implies that the neutrino  $N_1$  cannot contribute significantly to the active neutrino mass matrix. As we show below this conclusion is valid for all admissible masses and mixing angles.

Thus, at least three sterile neutrinos are required to account for DM and explain neutrino oscillations. In spite of the very weak coupling of DM sterile neutrino  $N_1$  with matter, it could have been produced in sufficient amounts in the early Universe (see Section 4.3 below).

### 3.3 Two heavier neutrinos

Two other sterile neutrinos ( $N_2, N_3$ ) should interact with the Standard Model particles more strongly than  $N_1$  to explain the observed pattern of neutrino oscillations. Here we outline properties of  $N_2$  and  $N_3$  upon which we elaborate further in Section 4.

The masses of these two sterile neutrinos should lie in the range  $150 \text{ MeV} \lesssim M_{2,3} \lesssim 100 \text{ GeV}$  and should be degenerate ( $\Delta M_{2,3} \ll M_{2,3}$ ). These characteristics are required for baryon asymmetry generation (Section 4.2). In order not to affect the predictions of big bang nucleosynthesis, we choose their masses and Yukawa couplings so that their lifetime  $\tau < 0.1 \text{ s}$  (i.e. they decay at temperatures  $T \gtrsim 3 \text{ MeV}$ ). These bounds are summarized in Figure 1.

The presence of these sterile neutrinos can affect DM production. If these particles decay *before* the DM is produced, they can generate significant lepton asymmetry. In the presence of lepton asymmetry sterile neutrino production proceeds differently [29]. If  $N_{2,3}$  decay *after* DM production, they heat the primordial plasma, increasing its entropy by a factor of  $S$  and changing its temperature by



$S^{1/3} > 1$ . As the DM sterile neutrinos decouple from the primeval plasma, they take no part in this entropy release, making their average momentum smaller than that of the active neutrinos by the same factor,  $S^{1/3}$ . As a result, the concentration of DM particles, compared to that of active neutrinos, decreases by a factor of  $S$ , and therefore the mixing angle, required to produce the same amount of DM particles *today*, becomes  $S$  times bigger for the same DM mass (compared to the  $S = 1$  case) [38]. *Therefore, the computation of sterile neutrino DM production and relation between the mass and mixing angle should be performed in the full  $\nu$ MSM, taking into account the influence of the neutrinos  $N_2, N_3$ .*

## 4 The $\nu$ MSM cosmology

In this section we describe the history of the Universe in the  $\nu$ MSM from inflation onward.

### 4.1 Inflation in the $\nu$ MSM

It has been shown [15] that it is possible to incorporate inflation within the  $\nu$ MSM approach, that is without introducing new particles above the electroweak scale. The role of the inflaton is played by the SM Higgs field  $\phi$ . The non-minimal coupling of  $\phi$  to the Ricci scalar  $R$

$$\mathcal{L}_R = \xi \phi^\dagger \phi R, \quad (13)$$

leads to a sufficiently flat effective potential for large values of  $\phi$ . The constant  $\xi$  is fixed by the Higgs mass and by the amplitude of scalar fluctuations, obtained from COBE's observations of the cosmic microwave background (CMB). For the SM model to be a consistent field theory all the way up to the Planck scale, the mass of the Higgs boson must lie in the interval  $126 \text{ GeV} < M_H < 194 \text{ GeV}$  [15, 39, 40] (see also [41, 42]). For uncertainties in these estimates see [40]. After inflation the Universe heats up to the temperature  $T = T_{\text{reh}} > 1.5 \times 10^{13} \text{ GeV}$ , creating all of the particles included in the SM. However, the singlet fermions of the  $\nu$ MSM are not created either during inflation or during reheating of the Universe because of the small values of their Yukawa couplings [43].

### 4.2 Baryon asymmetry of the Universe

Let us consider the stage of the Universe's evolution between the reheating temperature of  $\sim 10^{13} \text{ GeV}$  and the temperatures of  $\sim 100 \text{ GeV}$ . Our Universe is baryon asymmetric – it does not contain antimatter in amounts comparable with

matter, to wit:

$$\eta_B \equiv \frac{n_B}{s} = (8.8 \pm 0.2) \times 10^{-11} \quad (14)$$

where  $s$  is the entropy density [44]. To produce baryon asymmetry of the Universe three conditions should be satisfied [45]: (a) Conservation of the baryon number should be violated, (b) CP symmetry should be broken, and (c) the corresponding processes should be out of thermal equilibrium. Although the SM fulfills all these requirements [25], it cannot produce BAU because there is no first-order electroweak phase transition with experimentally allowed Higgs boson masses [46]. In addition, the CP violation in Cabibbo–Kobayashi–Maskawa mixing of quarks is unlikely to lead to the observed value of BAU (14).

The only source of baryon number non-conservation in the  $\nu$ MSM (as in the SM) is the electroweak anomaly [25]. The field configurations important for baryon number non-conservation are known as *sphalerons* [47]. The sum of baryon and lepton numbers is not conserved at temperatures above  $T_{\text{sph}} \sim 100$  GeV [25], and the BAU can be generated from the lepton asymmetry at  $T > T_{\text{sph}}$ .

A detailed description of the system of singlet leptons and active fermions in the early Universe is necessarily quite complicated. The number of relevant zero-temperature degrees of freedom (three active neutrinos, three sterile neutrinos, and their antiparticles) is large, and the timescales of different processes can vary by many orders of magnitude. To understand the qualitative picture of the creation of the matter excess (see Refs. [5, 48] for a detailed quantitative discussion and [49] for the original proposal of baryogenesis in singlet-fermion oscillations), one must determine the reasons for departure from thermal equilibrium [45]. The singlet fermions, with their very weak couplings to the SM fields, play an important role. The production rate of  $N_I$  is of the order of

$$\Gamma_I \sim |F_I|^2 T, \quad (15)$$

where  $|F_I|^2 \equiv \sum_{\alpha} |F_{\alpha I}|^2$ . Because at  $T_{\text{reh}}$  singlet fermions were absent, the number of created singlet fermions at temperature  $T$  is of the order of

$$q(T) \equiv \frac{n_I}{n_{eq}} \sim \frac{|F_I|^2 M_0}{T}, \quad (16)$$

where  $n_{eq}$  is an equilibrium concentration at given temperature. The temperature-time relation is given by  $t = \frac{M_0}{2T^2}$ ,  $M_0 \simeq M_{Pl}/1.66\sqrt{g_{eff}}$ , where  $g_{eff}$  is the number of effectively massless degrees of freedom. The relation shown in Eq. (16) is valid only if  $q < 1$ . The singlet fermion equilibrates at temperature  $T_+$ , defined via  $q(T_+) \sim 1$ , as

$$T_+ \simeq |F_I|^2 M_0. \quad (17)$$

The phase-space density constraints, together with X-ray bounds (Section 3.2), place an upper bound on the Yukawa coupling of the  $N_1$  at  $|F_1|^2 < 10^{-21}$ . The relation (16) shows that  $N_1$  is irrelevant for baryogenesis because  $q_{N_1} \ll 1$  at all temperatures  $T \geq T_{\text{sph}}$ . In other words,  $N_1$  practically decouples from the plasma.

If for both  $N_2$  and  $N_3$   $q(T_{\text{sph}}) > 1$ ,  $N_2$  and  $N_3$  come to thermal equilibrium before  $T_{\text{sph}}$ . In this case, even if baryon asymmetry of the Universe were generated before equilibration, it would be destroyed in equilibrium reactions with participation of sphalerons and singlet fermions. If  $q(T_{\text{sph}}) \sim 1$ , the fermions approach thermal equilibrium at the electroweak epoch, exactly what is needed for effective baryogenesis. This requirement restricts the masses of  $N_{2,3}$  to the 1 – 100-GeV region. A detailed analysis of this condition, which accounts for numerical factors and complicated flavor structure of asymmetry has been performed [48]. It leads to a constraint (Figure 1) on the mass-mixing angle plane.

Let us turn now to the effects of CP violation. Although the Yukawa matrix of singlet fermions generally contains CP-violating phases, in the tree-level processes their effects cancel out. Any quantum loop, which is necessary for CP violation to show up, is parametrically suppressed by  $F_{2\alpha}^2, F_{3\alpha}^2$ , which are much smaller than  $\eta_B$  (cf. Eq. (9)). The only means of overcoming this factor is to have a resonance, which occurs when the masses of sterile neutrinos  $N_2$  and  $N_3$  are nearly degenerate.

Let  $\Delta M(T)$  be the mass difference between  $N_2$  and  $N_3$  (temperature dependent due to Higgs' vev  $T$  dependence and radiative corrections at high temperatures). The frequency of oscillations between  $N_2$  and  $N_3$  is given by

$$\omega \sim \frac{|M_2^2 - M_3^2|}{E_I} \sim \frac{M_2 \Delta M(T)}{T}, \quad (18)$$

where we take into account that the typical energy of a singlet fermion  $E_I \sim T$  and that  $\Delta M(T) \ll M_2 \approx M_3$ . If the rate of oscillations exceeds the rate of the Universe's expansion  $H(T)$ , the system is out of resonance, and no amplification of CP violation occurs. In the opposite case, CP violation has no time to develop. This allows us to determine the temperature  $T_B$  at which baryogenesis occurs:  $\omega \sim H(T_B)$ , which leads to [49, 5],

$$T_B \sim \left( M_I \Delta M(T) M_0 \right)^{1/3}. \quad (19)$$

The described mechanism is quite effective. The *maximal* baryon asymmetry  $\Delta_B \equiv \frac{n_B - n_{\bar{B}}}{n_B + n_{\bar{B}}} \sim 1$  (i.e.  $\eta_B \sim 10^{-2}$ ) is produced when  $T_B \sim T_{\text{sph}} \sim T_+$ , leading to  $\Delta M(T_B) \sim 0.01 \text{ eV} \left( \frac{1 \text{ GeV}}{M_I} \right)$ . It is important that interactions with plasma do not destroy the quantum-mechanical nature of oscillations of  $N_{2,3}$ , in other words that  $T_+ \lesssim T_B$ .

The overall qualitative picture is as follows: Coherent pairs of singlet fermions are constantly created in interactions with the electroweak plasma. These fermions oscillate in a CP violating manner. As a result the Universe develops lepton asymmetry in the active, left-handed sector. This asymmetry is converted to baryon asymmetry due to anomalous electroweak reactions with baryon number non-conservation.

Probably, the simplest way to deal with all these effects in a quantitative way is to use the equation for the density matrix  $\rho$  [50, 51, 49, 5]. In this case  $\rho$  is a  $12 \times 12$  matrix ( $12 = 3 \times 2 \times 2$  degrees of freedom for all active and sterile neutrino states). For the problem at hand, this equation can be simplified (for details see Refs. [5, 48]):

1. The rates of interactions between active neutrinos are much higher than the rate of the Universe's expansion. Therefore, coherent effects for active neutrinos are not essential, and the part of the general density matrix  $\rho$  related to active leptonic flavors can be replaced with equilibrium concentrations characterized by three dimensionless chemical potentials  $\mu_\alpha$  (the ordinary chemical potential divided by the temperature), giving the leptonic asymmetry in each flavor.
2. Active neutrinos acquire temperature dependent masses [52] that are much larger than those of singlet fermions. Therefore, all non-diagonal elements of the density matrix simultaneously involving the active and sterile states can be set to zero.
3. The DM neutrino  $N_1$  is completely decoupled from the system.

This leaves us with the  $2 \times 2$  density matrix  $\rho_N$  for singlet fermions  $N_2$  and  $N_3$ , the charge conjugated density matrix  $\bar{\rho}_N$  for corresponding antiparticles (opposite-chirality states, to be precise), and three chemical potentials  $\mu_\alpha$ . The corresponding equations can be written as [5, 48]:

$$i \frac{d\rho_N}{dt} = [\mathcal{H}, \rho_N] - \frac{i}{2} \{ \Gamma_N, \rho_N - \rho^{eq} \} + i \mu_\alpha \tilde{\Gamma}_N^\alpha, \quad (20)$$

$$i \frac{d\bar{\rho}_N}{dt} = [\mathcal{H}^*, \bar{\rho}_N] - \frac{i}{2} \{ \Gamma_N^*, \bar{\rho}_N - \rho^{eq} \} - i \mu_\alpha \tilde{\Gamma}_N^{\alpha*}, \text{ and} \quad (21)$$

$$i \frac{d\mu_\alpha}{dt} = -i \Gamma_L^\alpha \mu_\alpha + i \text{Tr} \left[ \tilde{\Gamma}_L^\alpha (\rho_N - \rho^{eq}) \right] - i \text{Tr} \left[ \tilde{\Gamma}_L^{\alpha*} (\bar{\rho}_N - \rho^{eq}) \right]. \quad (22)$$

Here,  $\mathcal{H} = p(t) + \mathcal{H}_0 + \mathcal{H}_{int}$  is the Hermitian effective Hamiltonian incorporating the medium effects on neutrino propagation;  $p(t)$  is the neutrino momentum, with  $\langle p(t) \rangle \sim 3T$  (we assume that all the neutral fermion masses are much smaller than the temperature);  $\mathcal{H}_0 = \frac{M^2}{2p(t)}$  (we include  $\Delta M_{IJ}$  to  $\mathcal{H}_{int}$ );  $\rho^{eq} = \exp(-p/T)$  is an equilibrium diagonal density matrix; and  $[ , ]$  ( $\{ , \}$ ) corresponds to the commutator (anti-commutator). In Eq. (22) there is no summation over  $\alpha$  and  $\Gamma_L^\alpha$  are real. The explicit expressions for the equilibration rates  $\Gamma_N$ ,  $\tilde{\Gamma}_N^\alpha$ ,  $\Gamma_L^\alpha$ ,  $\tilde{\Gamma}_L^\alpha$  via Yukawa couplings can be found in Ref. [5] for the case in which the temperature

is higher than the electroweak scale and in Ref. [48] for the case in which the temperature is smaller. These equilibration rates are all related to the absorptive parts of the two point functions for active or sterile neutrino states, and they contain a square of Yukawa couplings  $F_{\alpha I}$ . The real parts of the corresponding graphs, together with the mass-squared difference between  $N_2$  and  $N_3$  determine the effective Hamiltonian  $\mathcal{H}$ . For high temperatures  $T \gtrsim T_{\text{sph}}$  the equilibration processes are associated with Higgs,  $W$  and  $Z$  decays to singlet and active fermions, to corresponding inverse processes, and to  $t\bar{t} \rightarrow N\bar{\nu}$  scattering (where  $t$  is the top-quark). At smaller temperatures  $T \lesssim T_{\text{sph}}$  the rates are associated with  $W$  and  $Z$  exchange and with singlet-active mixing through the Higgs vev. The last terms in Eqs. (20) and (21), as well as Eq. (22) are crucial for the generation of lepton asymmetry (see [5, 48]). In the earlier work [49] the computations and qualitative discussion were based on incomplete kinetic equations, that lacked these terms.

Equations (20–22), supplemented by initial conditions  $\rho_N = \bar{\rho}_N = \mu_\alpha = 0$  fixed by inflation (Section 4.1), give a basis for the analysis of the baryon and lepton asymmetry generation. It has been shown in Refs. [5, 48] that the observed baryon asymmetry (14) can be generated in a wide range of parameters of the  $\nu$ MSM, provided  $N_{2,3}$  are sufficiently degenerate:

$$\Delta M(T_B) \sim \sqrt{|\Delta m_{\text{atm}}^2|} \times \left( \frac{M_2}{\text{GeV}} \right)^2 \times \begin{cases} 800, & \text{normal hierarchy} \\ 6400, & \text{inverse hierarchy} \end{cases} . \quad (23)$$

The generation of baryon asymmetry stops at the temperature of the sphaleron freeze-out  $T_{\text{sph}}$ . The generation of the lepton asymmetry may still occur at  $T < T_{\text{sph}}$  [48]. Moreover, the magnitude of low-temperature lepton asymmetry has nothing to do with baryon asymmetry and may exceed it by many orders of magnitude. Sufficiently large lepton asymmetry  $\Delta_L \equiv \frac{n_{\nu_e} - n_{\bar{\nu}_e}}{n_{\nu_e} + n_{\bar{\nu}_e}} > 10^{-3}$  can affect the production of the DM sterile neutrino (see Section 4.3).<sup>3</sup>

Two different mechanisms can lead to late lepton asymmetry generation. As discussed above, the singlet fermions enter into thermal equilibrium at  $T_+$ . As the temperature decreases below the electroweak scale, the rate of interactions of singlet fermions with plasma gets suppressed by the Fermi constant, and these fermions decouple at some temperature  $T_-$ , that is somewhat higher than their mass [48]. The lepton asymmetry can then be generated below  $T_-$  in their oscillations, just as the baryon asymmetry was created above the electroweak scale. Alternatively, the lepton asymmetry can be created via decays of  $N_{2,3}$ . The analysis [48] shows that large lepton asymmetries ( $\Delta_L > 10^{-3}$ ) can be produced, provided that the zero-temperature mass degeneracy of  $N_{2,3}$  is high enough:  $\Delta M(0) \lesssim 10^{-4} \sqrt{|\Delta m_{\text{atm}}^2|}$  (note, that  $\Delta M(0)$  can differ significantly from  $\Delta M(T_B)$ .) The

---

<sup>3</sup>We denote by  $n_{\nu_e}$  ( $n_{\bar{\nu}_e}$ ) the number density of the electron neutrino (antineutrino), and assume throughout the paper that the lepton asymmetry is flavor blind.

*maximal possible lepton asymmetry* that can be produced at  $T_-$  or during the decays of  $N_{2,3}$  is  $\Delta_L^{\max} = 4/(9 \times 2 + 4) = 2/11$ , where 4 is the total number of spin-states of  $N_{2,3}$  and 9 is the number of spin-states of three lepton generations. This degree of asymmetry can be attained if CP violation is maximal. Generation of the baryon asymmetry at the level shown in Eq. (14), together with the large lepton asymmetry, is possible for the singlet fermion masses in the  $\mathcal{O}(\text{GeV})$  range and  $|F_2| \sim |F_3|$ . Following the Refs. [48, 53] we characterize the lepton asymmetry as  $L_6 \equiv 10^6(n_{\nu_e} - n_{\bar{\nu}_e})/s$ . The value  $\Delta_L^{\max} = 2/11$  corresponds to  $L_6^{\max} \approx 700$ . This value is still considerably smaller than the upper limit, imposed by the big bang nucleosynthesis [54]  $L_6^{\text{BBN}} \approx 2500$ .

### 4.3 DM production in the $\nu\text{MSM}$

In the  $\nu\text{MSM}$  DM sterile neutrinos are produced in the early Universe due to their coupling to active neutrinos. An estimate of the rate of DM sterile neutrino production  $\Gamma_N$  at temperatures below the electroweak scale is given by [55]

$$\Gamma_N \sim \Gamma_\nu \theta_M^2(T) , \quad (24)$$

where  $\Gamma_\nu \sim G_F^2 T^5$  is the rate of active neutrino production, and where  $\theta_M(T)$  is a temperature- (and momentum-) dependent mixing angle:

$$\theta_1^2 \rightarrow \theta_M^2(T) \simeq \frac{\theta_1^2}{\left(1 + \frac{2p}{M_1^2}(b(p, T) \pm c(T))\right)^2 + \theta_1^2} . \quad (25)$$

Here [56]

$$b(p, T) = \frac{16G_F^2}{\pi\alpha_W} p(2 + \cos^2\theta_W) \frac{7\pi^2 T^4}{360}, \quad c(T) = 3\sqrt{2}G_F(1 + \sin^2\theta_W)(n_{\nu_e} - n_{\bar{\nu}_e}) , \quad (26)$$

where  $\theta_W$  is the weak mixing angle,  $\alpha_W$  is the weak coupling constant, and  $p \sim$  few  $T$  is the typical momentum of created DM neutrinos. The term  $c(T)$  in (25) is proportional to the *lepton asymmetry* and contributes with the opposite sign to the mixing of  $N_1$  with active neutrinos and antineutrinos.

If the term  $b(p, T)$  dominates  $c(T)$  for  $p \sim (2 - 3)T$  [which we refer to as non-resonant production *NRP*], the production rate (24) is strongly suppressed at temperatures above a few hundred MeV and peaks roughly at [28]

$$T_{\text{peak}} \sim 130 \left( \frac{M_1}{1 \text{ keV}} \right)^{1/3} \text{ MeV} , \quad (27)$$

corresponding to the temperature of the quantum chromodynamics crossover for keV scale sterile neutrinos. This complicates the analysis, because neither the

quark, nor the hadron description of plasma is applicable at these temperatures [57]. In the region of the parameter space  $(\theta_1, M_1)$ , as demonstrated by X-ray observations together with dSph constraints (Section 3.2)  $\Gamma_N(T_{peak}) \ll H(T_{peak})$ . In other words the DM sterile neutrinos were never in thermal equilibrium in the early Universe. This fact allows us to make first principle computation of their abundance via certain equilibrium finite temperature Green's functions computed in the SM without inclusion of right-handed fermions [57, 58, 53]. (See Refs. [31, 59, 60] for earlier computations of sterile neutrino DM abundance. The sterile neutrino oscillations in the medium were also considered in Ref. [61]).

The shape of the primordial momentum distribution of the NRP sterile neutrinos is roughly proportional to that of the active neutrinos [30]:

$$f_{N_1}(t, p) = \frac{\chi}{e^{p/T_\nu(t)} + 1}, \quad (28)$$

where the normalization  $\chi \sim \theta_1^2$  and where  $T_\nu(t)$  is the temperature of the active neutrinos. The true distribution of sterile neutrinos is in fact colder than that shown in Eq. (28). Specifically, the maximum of  $p^2 f_{N_1}(p)$  occurs at  $p/T_\nu \approx 1.5-1.8$  (depending on  $M_1$ ), as compared with  $p \approx 2.2T_\nu$  for the case shown in Eq. (28) [57, 58].

The NRP mechanism specifies a *minimal* amount of DM that will be produced for given  $M_1$  and  $\theta_1$ . The requirement that 100% of DM be produced via NRP places an *upper bound* on the mixing angle  $\theta_1$  for a given mass. This conclusion can only be affected by entropy dilution arising from the decay of some heavy particles below the temperatures given in Eq. (27) [38]. In the  $\nu$ MSM such dilution may occur due to the late decay of two heavier sterile neutrinos (see Section 3.3).

The production of sterile neutrino DM may substantially change in the presence of lepton asymmetry. If the denominator in Eq. (25) is small,

$$1 + 2p \frac{b(p, T) \pm c(T)}{M_1^2} = 0, \quad (29)$$

then resonant production (*RP*) of sterile neutrinos [29] occurs, analogous to the Mikheyev–Smirnov–Wolfenstein effect [62, 63]. In this case the dispersion relations for active and sterile neutrinos cross each other at some momentum  $p$ , determined from Eq. (29). This results in the effective transfer of an excess of active neutrinos (or antineutrinos) to the population of DM sterile neutrinos. The maximal amount of sterile neutrino DM that can be produced in such a way ( $n_{res}$ ) is limited by the value of lepton asymmetry:  $n_{res} \lesssim |n_{\nu_e} - n_{\bar{\nu}_e}|$ . The present DM abundance  $\Omega_{DM} \sim 0.2$  [44] translates into  $n_{res}/s \lesssim 10^{-6} \frac{\text{keV}}{M_1}$ , in other words *the resonant effects in production of sterile neutrinos are not essential for  $L_6 \lesssim 1$*  (for masses in the keV range).

Resonantly produced DM sterile neutrinos have spectra that significantly differ from those in the NRP case [29, 53]. As a rule, the primordial velocity distribution of RP sterile neutrinos contains narrow resonant (*cold*) and nonresonant (*warm*) components. The spectra for  $M_1 = 3$  keV for  $L_6 = 10, 16, 25$  are shown in Fig. 2a as functions of comoving momentum  $q = p/T_\nu$ . The non-resonant tails are self-similar for the same mass and for different lepton asymmetries, and for  $q \gtrsim 3$  they behave as rescaled NRP spectra [58] with the same mass. We term this rescaling coefficient *the fraction of the NRP component*  $f_{\text{NRP}}$ . The dependence of the average momentum  $\langle q \rangle$  on the mass and lepton asymmetry is shown in Fig. 2b.

#### 4.4 Big Bang Nucleosynthesis.

Decays of heavy singlet fermions  $N_{2,3}$  heat the primeval plasma and distorts the spectra of active neutrinos from their thermal values. If this distortion occurs around the time of BBN, it may significantly influence its predictions. It has been shown [64, 65] that if the lifetime of sterile neutrinos  $\tau_{2,3} < 0.1$  s (i.e. they decay at temperatures above  $\sim 3$  MeV), the decay products have enough time to thermalize without spoiling the nucleosynthesis. This requirement places a *lower* bound on the strength of Yukawa interactions  $F_{\alpha 2}$  and  $F_{\alpha 3}$  (Fig. 1) [66]. A detailed treatment of the decays of sterile neutrinos and their interaction with primordial plasma can somewhat change these constraints, in particular by allowing for smaller Yukawa couplings.

#### 4.5 Structure formation in the $\nu$ MSM

Comparing the production temperatures Eq. (27) of DM sterile neutrinos with their masses shows that they are produced relativistically in the radiation-dominated epoch. Relativistic particles stream out of the overdense regions and erase primordial density fluctuations at scales below the *free-streaming horizon* (FSH) – particles’ horizon when they becomes nonrelativistic. (For a detailed discussion of characteristic scales see e.g. [67] and references therein). This effect influences the formation of structures. If DM particles decouple nonrelativistically (*cold* DM models, CDM) the structure formation occurs in a “bottom-up” manner: specifically, smaller scale objects form first and then merge into the larger ones [68]. CDM models fit modern cosmological data well. In the case of particles, produced relativistically and *remaining relativistic* into the matter-dominated epoch (i.e. *hot* DM, HDM), the structure formation goes in a “top-down” fashion [69], where the first structures to collapse have sizes comparable to the Hubble size [70, 71, 72]. The HDM scenarios contradict large-scale structure (LSS) observations. Sterile neutrino DM are produced out of equilibrium at the temperatures shown in Eq. (27) and is then redshifted to nonrelativistic velocities in



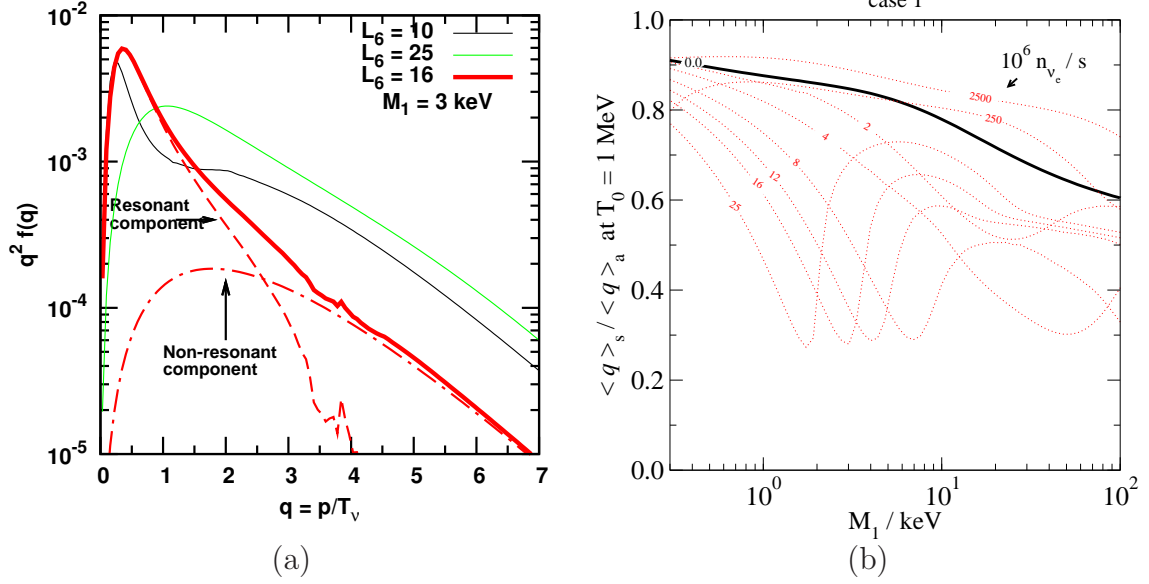


Figure 2: **(a)** Characteristic form of the resonantly produce (RP) sterile neutrino spectra for  $M_1 = 3$  keV and  $L_6 = 16$  (red solid line) and its resonant and non-resonant components. Also shown are spectra for  $L_6 = 10$  and  $L_6 = 25$ , all of which have the same form for  $q \gtrsim 3$ . All spectra are normalized to give the same DM abundance. For the spectrum with  $L_6 = 16$ , its nonresonantly produce (NRP) component  $f_{\text{NRP}} \simeq 0.12$  ((red dashed-dotted line) and its colder, RP component (red dashed line) are shown separately. The spectrum with  $L_6 = 10$  has  $f_{\text{NRP}} \simeq 0.53$  and  $L_6 = 25$  has  $f_{\text{NRP}} \simeq 0.60$ . The RP components happen to peak around  $q_{\text{res}} \sim 0.25 - 1$ . Their width and height depends on  $L_6$  and  $M_1$ . **(b)** Dependence of the ratio of the average momentum of sterile neutrinos to that of the active neutrinos on mass  $M_1$  and lepton asymmetry. The black solid curve represents the ratio of average momenta, computed over the exact NRP spectra to the ratio using the approximate analytic form shown in Eq. (28). The black solid curve is the ratio of average momenta, computed over exact NRP spectra to the ratio, computed using the approximate analytic form (28). For each mass there is lepton asymmetry for which the  $\langle q \rangle$  reaches its minimum  $\langle q \rangle_{\text{min}} \sim 0.3 \langle q \rangle_{\nu_\alpha}$ . The corresponding spectra are the most distinct from the NRP spectra. The fraction  $f_{\text{NRP}}$  for the former can be  $\lesssim 20\%$ . Panel **b** reproduced from Ref. [53] with permission.

the radiation-dominated epoch (*warm* DM, WDM). Structure formation in WDM models is similar to that in CDM models at distances above the free streaming scale. Below this scale density fluctuations are suppressed, compared with the CDM case. The free-streaming scale can be estimated as [71]

$$\lambda_{\text{FS}}^{\text{co}} \sim 1 \text{ Mpc} \left( \frac{\text{keV}}{M_1} \right) \frac{\langle p_N \rangle}{\langle p_\nu \rangle}. \quad (30)$$

where 1 Mpc is the (comoving) horizon at the time when momentum of active neutrinos  $\langle p_\nu \rangle \sim 1 \text{ keV}$ . If the spectrum of sterile neutrinos is nonthermal, then the non-relativistic transition and  $\lambda_{\text{FS}}^{\text{co}}$  shift by  $\langle p_N \rangle / \langle p_\nu \rangle$ . To account for the influence of primordial velocities on the evolution of density perturbations, it is convenient to introduce a *transfer function* (TF) with respect to the CDM model,

$$T(k) \equiv [P_{\text{WDM}}(k)/P_{\text{CDM}}(k)]^{1/2} \leq 1. \quad (31)$$

where the power spectra  $P_{\text{WDM}}(k)$  and  $P_{\text{CDM}}(k)$  are computed with the same cosmological parameters. In general, the characteristic shape of a TF depends upon a particular WDM model. In the  $\nu$ MSM the TF's shape is determined by the mass of DM particle and lepton asymmetry, which define the primordial velocity distribution. In the case of both RP and NRP sterile neutrino, the TF starts to deviated from one for  $k \gtrsim k_{\text{FSH}}^0$ , where

$$k_{\text{FSH}}^0 = 0.5 \left( \frac{M_1}{1 \text{ keV}} \right) \left( \frac{0.7}{h} \right) \left( 1 + 0.085 \ln \left[ \left( \frac{0.1}{\Omega_M h^2} \right) \left( \frac{M_1}{1 \text{ keV}} \right) \right] \right)^{-1} h/\text{Mpc}. \quad (32)$$

is a *free-streaming horizon* for a model with mass  $M_1$  and the velocity distribution in Eq. (28) (c.f. [67]). In Eq. (32)  $\Omega_M$  is the total matter density, and  $H_0 = h \times 100 \text{ km s}^{-1} \text{ Mpc}^{-1}$  is the Hubble constant today. For  $k \gg k_{\text{FSH}}^0$  the TF of NRP sterile neutrinos falls off as  $\sim k^{-10}$  (c.f. [73, 74, 67]). For the TF of RP sterile neutrinos we define  $k_{\text{FSH}}^{\text{res}} \simeq k_{\text{FSH}}^0 \langle q \rangle / q_{\text{res}}$ . For scales  $k \leq k_{\text{FSH}}^{\text{res}}$  the  $T_{\text{RP}}(k)$  is indistinguishable from that of cold-plus-warm dark matter (the mixture of the WDM component in the form of NRP sterile neutrinos and pure CDM) with the same mass and the same fraction of the warm component  $F_{\text{WDM}} = f_{\text{NRP}}$ . For smaller scales ( $k > k_{\text{FSH}}^{\text{res}}$ ) the  $T_{\text{RP}}(k)$  decays, because the cold component of RP sterile neutrinos also has a nonnegligible free-streaming, determined roughly by  $k_{\text{FSH}}^{\text{res}}$ . This characteristic behavior of NRP and RP spectra is demonstrated in Fig. 3. We discuss cosmological restrictions on the sterile neutrino DM models in Section 5.1.3.

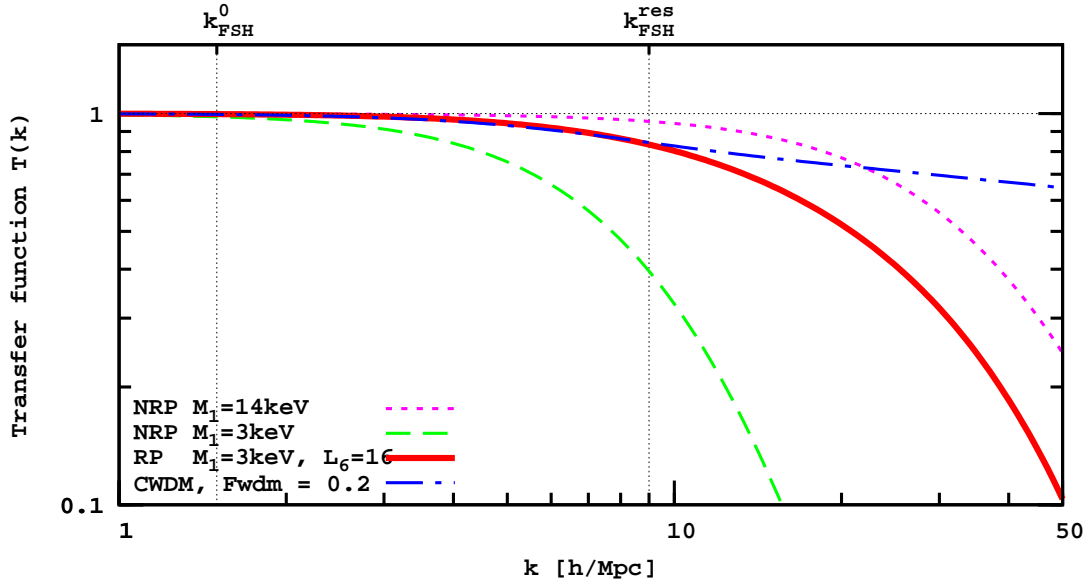


Figure 3: Transfer functions (TFs) for the nonresonant production (NRP) spectra where  $M_1 = 14$  keV and  $M_1 = 3$  keV. Also shown is a resonant production (RP) spectrum where  $M_1 = 3$  keV and  $L_6 = 16$  together with a cold/warm DM spectrum for  $M = 3$  keV and  $F_{\text{WDM}} \simeq 0.2$  (blue dashed-dotted line). Vertical lines mark the free-streaming horizon of the nonresonant ( $k_{\text{FSH}}^0$ , left line) and resonant ( $k_{\text{FSH}}^{\text{res}}$ , right line) components. Abbreviations: CWDM, cold-plus-warm dark matter; WDM, warm dark matter.

## 5 Search for $\nu$ MSM physics

### 5.1 Combined Restrictions from Astrophysics

Below we summarize the astrophysical bounds on the sterile neutrino dark matter.

#### 5.1.1 Phase-space density bounds.

The most robust *lower bound* on the DM mass comes from the analysis of the phase-space density of compact objects such as dwarf spheroidal galaxies of the Milky Way. The universal Tremaine-Gunn bound [33] can be strengthened if one **(a)** knows the primordial velocity distribution of the DM particles and **(b)** takes into account that the dynamics of DM particles is collisionless and dissipationless and that an initial phase-space volume occupied by DM particles is therefore preserved in the course of evolution. (For further discussion, see, e.g., [34, 75, 76] and references therein). For the NRP sterile neutrino, this leads to  $M_1 > 1.8$  keV [34]. For the same mass, the primordial velocity distribution of RP sterile neutrino DM is colder than the NRP dark matter. Analysis of available spectra shows that models in which  $M_1 > 1$  keV are allowed for most values of lepton asymmetries [34]. Note, however, that in derivation of these bounds (unlike the bound, based on the Pauli exclusion principle) the presence of dissipative baryons was not taken into account. However, because dSphs are the most dark and DM-dominated objects (with a mass-to-light ratio  $> 100M_\odot/L_\odot$ ), we expect the results of Ref. [34] to be robust.

#### 5.1.2 X-ray constraints.

Because the sterile neutrino is a decaying DM candidate, its decays would produce a narrow line in spectra of DM-dominated astrophysical objects [30, 32]. The width of this line is determined by the virial motion of DM particles in halos. It ranges from  $\Delta E/E \sim 10^{-2}$  for galaxy clusters to  $10^{-4}$  for dSphs. The expected flux of the DM decay is given by

$$F_{\text{DM}} = \frac{M_{\text{DM}}^{\text{fov}} \Gamma}{4\pi D_L^2} \frac{E_\gamma}{M_1} \simeq 6.38 \left( \frac{M_{\text{DM}}^{\text{fov}}}{10^{10} M_\odot} \right) \left( \frac{\text{Mpc}}{D_L} \right)^2 \times \sin^2(2\theta_1) \left[ \frac{M_1}{\text{keV}} \right]^5 \frac{\text{keV}}{\text{cm}^2 \cdot \text{sec}}, \quad (33)$$

where  $M_{\text{DM}}^{\text{fov}}$  is the mass of DM within a telescope's field of view (FoV), the decay rate  $\Gamma$  is given by Eq.(33) and  $D_L$  is the luminous distance to the object. Eq. (33) is valid in nearly all interesting cases apart from that of the signal from the Milky Way halo (c.f. [77, 78]). We begin our discussion of X-ray constraints with considering the mass range  $0.4 \text{ keV} \lesssim M_1 \lesssim 30 \text{ keV}$  with corresponding photon energy  $E_\gamma = M_1/2$  falling into the X-ray band. Modern X-ray instruments have a FoV of

$\sim 10' - 15'$  which is below the characteristic scale of DM distribution in a large variety of objects. As a result, the DM density does not change significantly within the instrument's FoV, and the DM flux (33) is determined by the *DM column density*  $\mathcal{S} = \int \rho_{\text{DM}}(r) dr$ :

$$F_{\text{DM}} = \frac{\Gamma \Omega_{\text{fov}}}{8\pi} \int_{\text{line of sight}} \rho_{\text{DM}}(r) dr . \quad (34)$$

Note, that in this limit the expected signal does not depend on the distance to the object. Instead, it is determined by the angular size  $\Omega_{\text{fov}}$  and the DM overdensity  $\mathcal{S}$ . The central DM column density is comparable (within a factor  $\sim 10$ ) for most of DM-dominated objects of different types and scales. The objects with the highest column densities are central regions of dSphs (such as Ursa Minor or Draco) and of Andromeda galaxy. The expected signals from these objects are a few times stronger than that of the Milky Way halo (through which one observes all the objects). However there are a variety of objects, covering the FoV of an X-ray instrument, that would produce comparable signals (in contrast with signals from annihilating DM). This gives us a certain freedom to choose observational targets, that may be exploited in two ways (described below). Galaxies and galaxy clusters are X-ray bright objects whose spectra contain many atomic lines. The DM decay line should be distinguished from these lines (and from those of the instrumental origin). One can reliably identify atomic lines in cases where several of them originate from transitions in the same element and therefore have known relative intensities. The emission of hot gas (including the positions and intensities of lines) can be described by models with a few parameters such as abundances of elements. Another way to distinguish an unidentified astrophysical line from the DM decay line is to study its surface-brightness profile. The surface brightness profiles of atomic lines are proportional to the gas density squared, while the surface brightness profile of a DM line is proportional to the density. To avoid complicated modeling and related uncertainties, one can analyze dark outskirts of extended objects (such as clusters [79] or big galaxies [80]) or search for a line against a featureless astrophysical background such as the extragalactic X-ray background [81, 77, 78, 82]. The best strategy is to look in the spectra of X-ray quiet and DM dominated objects, in particular dSphs [77, 78]. Extensive searches for these lines have been performed using *XMM-Newton* [81, 79, 77, 83, 78, 84, 80], *Chandra* [85, 83, 86, 82], *INTEGRAL* [87, 88], and *Suzaku* [89]. They did not reveal any ‘‘candidate’’ line in the energy range from  $\sim 0.5$  keV to about 14 MeV. These searches yielded an upper bound on the possible DM flux. To convert it to the upper bound on the mixing angle (via Eq. (11)), one must reliably determine the amount of DM in the observed objects. Determining the amount of DM in any given object is subject to specific systematic uncertainties, related

e.g. to assumptions about the spherical symmetry of the DM halo, modeling of the contribution of baryons to the rotation curves, and assumptions about the hydrostatic equilibrium of intra-cluster gas, etc (see e.g. [86, 80, 88]). Therefore, it is important to rule out the same parameter values from several targets (preferably of different scale and nature).

The bounds obtained from the combined results of these searches (Figure 4) are based on independent results from various objects (extragalactic X-ray background [81, 77], the Milky Way [77, 85, 78, 84, 82, 87, 88], M31 [83, 80], galaxy clusters [79, 86], and dSph galaxies [78, 89]). Superposing several results makes them robust. Comparing the of production curves (i.e. the relations between  $\theta_1$  and  $M_1$ , which produce the required DM abundance) with the bounds on DM decay flux leads to the upper mass bound. In the NRP case, the *upper bound* on the DM sterile neutrino mass was found to be  $M_1 \leq 4$  keV [80]. For a more effective RP scenario, the smaller mixing angles are admissible, and the corresponding mass bound is much weaker:  $M_1 \lesssim 50$  keV [53, 34].

To improve the modern astrophysical bounds (Fig. 4) with existing instruments, one should conduct prolonged (several Msec) observations of dSph galaxies and other X-ray quiet objects, then combine various observations. The bounds would improve roughly as  $T_{\text{exp}}^{1/2}$  with cumulative exposure time.

A real improvement in sensitivity can be achieved with the next generation of X-ray spectrometers which will have an energy resolution  $\Delta E/E \sim 10^{-3}$ – $10^{-4}$  and which will maximize the product of their effective area and FoV. For a comparison of the sensitivities of existing and future missions, see Ref. [84, 91]. For an example of a spectrometer with optimal characteristics for performing a decaying DM search see e.g. [92, 91]. Such a mission would allow us to improve the sensitivity towards the DM search by up to a factor of  $10^3$ . Its preferred observational targets would be our Galaxy, its dwarf satellites, and galaxy clusters.

If a candidate line is found, its surface-brightness profile can be measured, distinguished from astrophysical lines, and compared with those of several objects with the same expected signal. This would make an astrophysical search for decaying DM *another type of a direct detection experiment*.

### 5.1.3 Lyman- $\alpha$ constraints.

Below we describe the Lyman-alpha method and the Lyman-alpha constraints on the properties of warm and cold-plus-warm dark matter models and in particular sterile neutrino dark matter.

**Structure formation at different scales.** The sterile neutrino DM creates a cut-off in the power spectrum of matter density fluctuations at sub-Mpc scales. At larger scales, the power spectrum can be determined by CMB experiments,

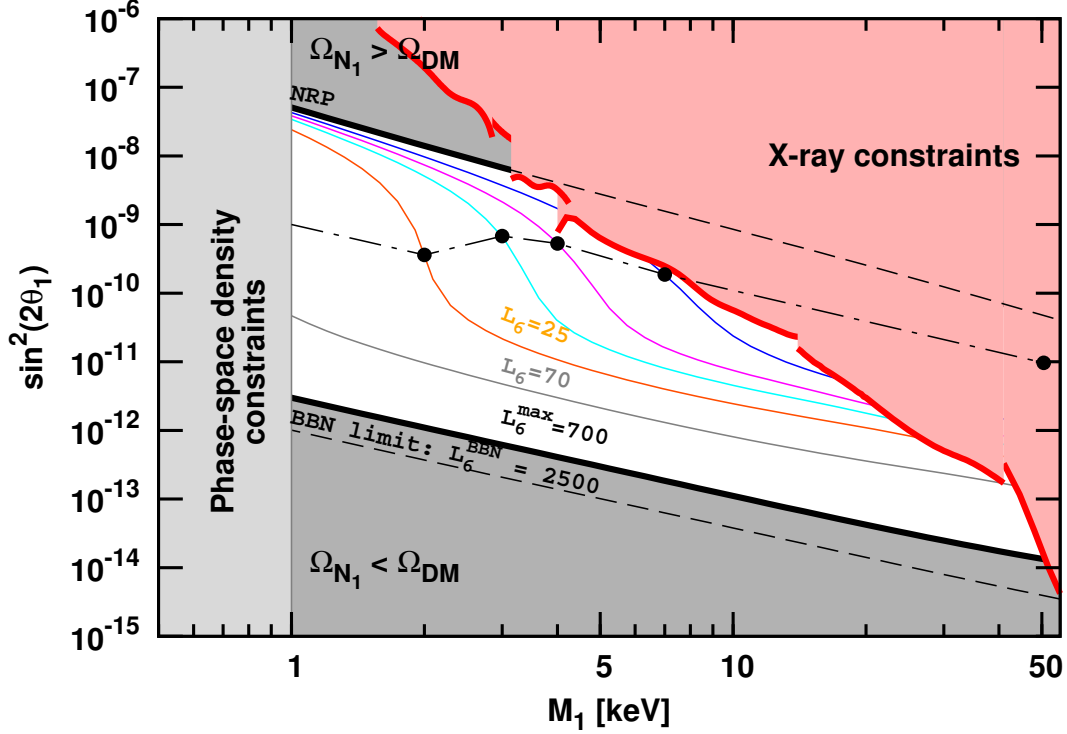


Figure 4: The allowed region of parameters for DM sterile neutrinos produced via mixing with the active neutrinos (*unshaded region*). The two thick black lines bounding this region represent production curves for nonresonant production (NRP) (*upper line*,  $L_6 = 0$ ) and for resonant production (RP) (*lower line*,  $L_6^{\max} = 700$ ) with the maximal lepton asymmetry, attainable in the  $\nu$ MSSM [53, 48]. The thin colored curves between these lines represent production curves for (*from top to bottom*)  $L_6 = 8, 12, 16, 25$ , and  $70$ . The red shaded region in the upper right corner represents X-ray constraints [77, 78, 80, 88, 89] (rescaled by a factor of two to account for possible systematic uncertainties in the determination of DM content [86, 80]). The black dashed-dotted line approximately shows the RP models with minimal  $\langle q \rangle$  for each mass, i.e., the family of models with the largest cold component. The black filled circles along this line are compatible with the Lyman- $\alpha$  bounds [90], and the points with  $M_1 \leq 4$  keV are also compatible with X-ray bounds. The region below 1 keV is ruled out according to the phase-space density arguments [34]. Abbreviation: BBN, big bang nucleosynthesis.

or reconstructed from observed galaxy power spectrum (via LSS surveys). For any mass and mixing angle that satisfies the constraints named above, the *sterile neutrino DM model fits the CMB and LSS data* as well as the  $\Lambda$ CDM “concordance model”. One of the main probes of the matter power spectrum at sub-Mpc scales is the *Lyman- $\alpha$  forest method*, discussed below.

**Lyman- $\alpha$  method.** It has been well established by analytical calculations and hydrodynamical simulations that Lyman- $\alpha$  absorption lines in spectra of distant quasars are produced by clouds of neutral hydrogen at different redshifts along the line of sight. This neutral hydrogen is part of the warm ( $\sim 10^4$ -K) and photoionized intergalactic medium. Opacity fluctuations in the spectra arise from fluctuations in the neutral hydrogen density, which can be used to trace cosmological fluctuations on scales  $k \sim (0.1 - 5) h \text{ Mpc}^{-1}$ , at redshifts  $z \sim 2 - 4$ . Thus it is possible to infer fluctuations in the total matter distribution [93, 94, 95]. For each quasar, the observed spectrum  $I(z)$  can be expanded in (one-dimensional) Fourier space. The expectation value of the squared Fourier spectrum is known as the *flux power spectrum*  $P_F(k)$ .

The flux power spectrum  $P_F(k)$  is a complicated function of the cosmological parameters. In the range of scales probed by Lyman- $\alpha$  data, the effects of free-streaming may be compensated for by a change in other cosmological parameters. Therefore, it is important to perform collective fits to the Lyman- $\alpha$  data and to CMB and LSS data. At redshifts and scales probed by Lyman- $\alpha$ , the fluctuations already enter into a mildly non-linear stage of gravitational collapse ( $\delta\rho/\rho \gtrsim 1$ ). To predict  $P_F(k)$  for a given cosmological model, one must perform hydrodynamical simulations: for CMB experiments probing the linear matter power spectrum, it is sufficient to compute the evolution of linear cosmological perturbations using a Boltzmann code such as CAMB [96]). Hydrodynamical simulations are necessary both for simulating the non-linear stage of structure formation and for computing the evolution of thermodynamical quantities (so as relate the non-linear matter power spectrum to the observable flux power spectrum). In principle, to fit Lyman- $\alpha$  data one should perform a full hydrodynamical simulation for each cosmological model. This is computationally prohibitive, and various simplifying approximations have been proposed [97, 98, 99, 100, 74, 101, 102, 103]. Although potentially very powerful, the Lyman- $\alpha$  method is indirect and hinges on a large number of assumptions (see e.g. [67]).

**Lyman- $\alpha$  bounds.** A Lyman- $\alpha$  analysis [104, 74, 105, 106, 107] has been performed for NRP mechanism of sterile neutrinos, assuming a model with only one sterile neutrino. The bounds [74, 106, 105] were recently revised in Ref. [67], who used the same SDSS Lyman- $\alpha$  data [99] combined with WMAP5 data [44]), and



paying special attention to the interpretation of statistics in the parameter extraction and to possible systematic uncertainties. It was shown that a conservative (i.e. frequentist,  $3\text{-}\sigma$ ) lower bound is  $M_1 > 8$  keV. The Lyman- $\alpha$  method is still under development, and there is a possibility that some of the related physical processes are not yet fully understood. However, it is difficult to identify a source of uncertainty that could give rise to systematic errors affecting the result by more than 30%. Even with such an uncertainty, the possibility of all DM being in the form of NRP sterile neutrinos can be ruled out by comparing Lyman- $\alpha$  results with X-ray upper bounds [67].

A full Lyman- $\alpha$  analysis of DM models containing both resonant and non-resonant components has not yet been conducted. However in [67] a cold-plus-warm DM model (CWDM) has been analyzed. Although the phase-space distribution of RP sterile neutrinos does not coincide exactly with such mixed models, some results can be inferred from the CWDM analysis. In particular, it has been shown [90], that the cosmological signature of RP sterile neutrino DM can be approximated by that of CWDM. With these results [67], it was shown that for each mass  $M_1 \geq 2$  keV, there exists at least one model of sterile neutrino that can account for the totality of dark matter, and that is consistent with Lyman- $\alpha$  and other cosmological data. These corresponding values of lepton asymmetry can be obtained within the  $\nu$ MSM.

#### 5.1.4 Galaxy substructures.

The suppression of the matter power spectrum at sub-Mpc scales may affect galaxy substructures. Qualitatively one expects a cut-off scale for the existence of DM substructures in the Milky Way-type galaxies. The primordial velocities of DM particles do not allow them to move too close together, thereby creating shallow density profiles. Quantitative conclusions about the mass function of dwarf satellites and slopes of density profiles of galactic substructures require numerical simulations, as the galaxy formation today is at a non-linear stage.

A number of studies have claimed discrepancies between astrophysical observations and CDM numerical simulations of galaxy formation (see e.g. [108, 109, 110, 111, 73]). For example:

1. The number of observed dSphs of the Milky Way is still more than an order of magnitude below the CDM predictions, in spite of the drastically improved sensitivity in the dSphs search (see e.g. [112, 113]);
2. direct measurements of DM density profiles in dSphs seem to favor cored profiles [114, 115, 116, 112];
3. there may be indications of the existence of the smallest scale at which DM is observed [112, 117].

However, it is not clear whether a ‘‘CDM substructure crisis’’ exists. Various

astrophysical resolutions of such a crisis has been proposed (see e.g. [118, 119, 120, 121, 122, 123, 124, 125]). It is extremely challenging to verify these resolutions both experimentally and numerically because the full-scale numerical simulations including baryons and their feedback on structure formation are not currently possible. To understand how galaxy structure formation occurs in the WDM models, one must perform numerical simulations, that take into account thermal velocities of DM particles (see e.g. [126], [67]).

## 5.2 Particle physics experiments

Because many of the parameters of the  $\nu$ MSM are fixed or constrained by experiments on neutrino masses and oscillations, as well as by cosmological considerations, it is possible to rule out or to confirm this model.

We list below the  $\nu$ MSM predictions for experiments that are under way or that will be carried out in the near future.

1. Nothing but the Higgs boson within the mass interval  $126 \text{ GeV} < M_H < 194 \text{ GeV}$  will be found at the LHC [127, 43, 39, 40] (uncertainties in these numbers are given in [40]).

2. One of the active neutrinos in the  $\nu$ MSM must be very light,  $m_1 \lesssim \mathcal{O}(10^{-6}) \text{ eV}$  [4, 128], which fixes the masses of the two other active neutrinos at  $m_2 \simeq 9 \cdot 10^{-3} \text{ eV}$  and  $m_3 \simeq 5 \cdot 10^{-2} \text{ eV}$  for normal hierarchy or  $m_{2,3} \simeq 5 \cdot 10^{-2} \text{ eV}$  for the inverted hierarchy. As a result, an effective Majorana mass for neutrinoless double-beta decay can be determined [129]. For normal (inverted) hierarchy the constraints are  $1.3 \text{ meV} < m_{\beta\beta} < 3.4 \text{ meV}$  ( $13 \text{ meV} < m_{\beta\beta} < 50 \text{ meV}$ ).

3. There will be negative results for the direct and indirect searches for weakly interacting massive particles, proton decay, neutron oscillations, and extra sources of CP-violation in the hadronic sector.

Although the experiments listed above can rule out the  $\nu$ MSM, they cannot provide its direct confirmation. We can only obtain confirmation if all three singlet fermions are discovered. Astrophysical searches for the DM sterile neutrino are described at length above. Laboratory searches for this particle would require a challenging, detailed analysis of the kinematics of  $\beta$ -decays of different isotopes [130]. A pair of new neutral leptons, creating the baryon asymmetry of the universe, can be searched for [66] in dedicated experiments that use existing intensive proton beams at CERN, FNAL, and planned neutrino facilities in Japan (J-PARC). Alternatively, one can look for a specific missing energy signal in  $K$ ,  $D$ , and  $B$  decays. In general, the  $\nu$ MSM paradigm tells us that to uncover new phenomena in particle physics we should utilize high-intensity proton beams with fixed-target experiments or to very high intensity charm or B-factories, rather than high energy accelerators.

## 6 Conclusion

Sterile neutrinos may play a key role in resolving the BSM problems. For the specific choice of parameters described above, they can explain the neutrino flavor oscillations and the origin of the matter-antimatter asymmetry in the Universe, and can provide a DM candidate. Sterile neutrino DM can be cold or warm, affecting the formation of structures at sub-Mpc scales. This parameter choice does not contradict existing experimental bounds and it assumes masses below the electroweak scale. This means that sterile neutrinos can be searched for in existing accelerator and laboratory experiments. The parameter space of the sterile neutrinos in the  $\nu$ MSM is bounded from all sides, allowing for verification or falsification of this model.

**Beyond the  $\nu$ MSM.** The  $\nu$ MSM is a minimal theory that can address the SM problems in a unified way. Of course, the fact that it is minimal does not mean that it is correct. Even if the low-energy electroweak theory indeed contains three relatively light neutral right-handed leptonic states, the full theory may be much more complicated. Extending the  $\nu$ MSM at low or high energies will change the predictions of this model. For example, introducing the low-energy supersymmetry would add another DM candidate to the theory, allowing wider variation of the parameters of DM sterile neutrinos. If GUT theories are proven to be true, they would introduce another source of baryon number non-conservation, leading to a different origin of BAU.

Finally, we briefly discuss two modest modifications of the  $\nu$ MSM. In the first, one adds to the Lagrangian (5) the higher-dimensional operators given in Eq. (1). This allows for production of DM sterile neutrinos at reheating after inflation [43], provided that they are heavier than 100 keV. This does not contradict to X-ray constraints because the mixing angle  $\theta_1$  is not essential for this production mechanism. The sterile neutrino, in this case, can only play the role of CDM candidate.

The second modification of the  $\nu$ MSM requires the addition of a singlet scalar field [131]. This field may give a mass to singlet fermions due to Yukawa couplings to these fermions, and it may play the role of the inflaton [131, 132]. The decays of this scalar to DM sterile neutrinos may serve as an efficient mechanism of cold or warm DM production, without conflicting with X-ray constraints [131, 133, 134, 135, 136]. In such models the mass of sterile neutrino DM can be in the MeV range or even in the GeV range. The radiative decays of such DM particles can be searched for with *Fermi* (cf. [137]), whose large FoV requires a new search strategy.

**Astrophysical applications of sterile neutrinos.** A final word about astrophysical applications of right-handed neutrinos, discussed in this work. The mean free path of a sterile neutrino inside a collapsing star is much larger than that of an ordinary neutrino. The escape of sterile neutrinos from the supernova may thus provide an effective cooling mechanism. For sterile neutrinos with the masses  $M \gtrsim 10^2$  keV the analysis of the data from the supernova 1987A leads to an upper bound on the mixing with electron neutrino  $\sin^2(2\theta_e) \lesssim 10^{-10}$  [138, 139, 140, 141]. In the case of sterile neutrinos with the mass  $M < 10^2$  keV the analysis shows that the mixing with the electron neutrinos is bounded by  $\sin^2(2\theta_e) \lesssim 10^{-8} \left(\frac{\text{keV}}{M}\right)^2$  for  $1 \text{ keV} \lesssim M \lesssim 100 \text{ keV}$  [139, 142], while the mixing with  $\nu_{\mu,\tau}$  is bounded by  $\sin^2(2\theta_{\mu,\tau}) \lesssim 3 \times 10^{-8} T_{30}^{-6}$  [64] (c.f. [31]) where  $T_{30} = T_{\text{core}}/30$  MeV and a typical supernovae core temperatures,  $T_{\text{core}}$ , lie in the range 20 – 70 MeV [143]. Owing to large uncertainties in the supernova physics, the constraints on the mixing angle of the sterile neutrino that arise from these considerations happen to be weaker than the X-ray bounds discussed above (Section 5.1.2) [64, 65].

At the same time, the analysis of [144, 145] shows that sterile neutrinos with the masses  $1 \text{ keV} \lesssim M \lesssim 5 \text{ keV}$  and with the mixing angle with  $\nu_e$   $10^{-10} \lesssim \sin^2(2\theta_e) \lesssim 10^{-8}$  may enhance lepton number, energy, and entropy transport in supernovae explosions. The results of [146] indicate that sterile neutrinos with the mass  $M_{2,3} \sim 200$  MeV and mixing angles  $\theta_7^2 > 10^{-8}$  or  $10^{-8} < \theta_\mu^2 < 10^{-7}$  can augment shock energies of core collapse supernovae. The asymmetric emission of keV sterile neutrinos from a supernova explosion may lead to an explanation of pulsar kick velocities [147, 148, 149, 133, 134, 150], see [151] for a review. The X-ray photons from early decays of these particles can influence the formation of molecular hydrogen and can be important for the early star formation and re-ionization [152, 153, 154, 155, 156]. See also Refs. [157, 158, 159] for a discussion of the formation of super-massive black holes and degenerate heavy neutrino stars.

Finally, if DM consists of many components (as may occur in extensions of the  $\nu$ MSM) such that sterile neutrinos constitute only a fraction  $f < 1$  of it, the X-ray bounds shown in Fig. 4 become weaker by the same factor. Moreover, the Lyman- $\alpha$  constraints also become diluted [160, 67], if the rest of DM is cold. The analysis in [67] shows that the DM sterile neutrino with the spectrum given by Eq. (28) and a mass  $M_1 \geq 5$  keV for  $f < 0.6$  satisfies all existing constraints at 99.7% CL. Once  $f < 1$ , sterile neutrino effects in astrophysics may be even more important.

## Acknowledgments

O.R. and M.S. acknowledge support of Swiss National Science Foundation.

## References

- [1] S. L. Glashow, Nucl. Phys. **22**, 579 (1961).
- [2] S. Weinberg, Phys. Rev. Lett. **19**, 1264 (1967).
- [3] A. Salam, (1968), Originally printed in \*Svartholm: Elementary Particle Theory, Proceedings Of The Nobel Symposium Held 1968 At Lerum, Sweden\*, Stockholm 1968, 367-377.
- [4] T. Asaka, S. Blanchet, and M. Shaposhnikov, Phys. Lett. **B631**, 151 (2005), hep-ph/0503065.
- [5] T. Asaka and M. Shaposhnikov, Phys. Lett. B **620**, 17 (2005), hep-ph/0505013.
- [6] A. Strumia and F. Vissani, (2006), hep-ph/0606054.
- [7] C. Giunti, Nucl. Phys. Proc. Suppl. **169**, 309 (2007), hep-ph/0611125.
- [8] T. Schwetz, M. Tortola, and J. W. F. Valle, New J. Phys. **10**, 113011 (2008), 0808.2016.
- [9] MINOS, P. Adamson *et al.*, Phys. Rev. Lett. **101**, 131802 (2008), 0806.2237.
- [10] KamLAND, S. Abe *et al.*, Phys. Rev. Lett. **100**, 221803 (2008), 0801.4589.
- [11] P. Minkowski, Phys. Lett. **B67**, 421 (1977).
- [12] P. Ramond, (1979), hep-ph/9809459.
- [13] R. N. Mohapatra and G. Senjanovic, Phys. Rev. Lett. **44**, 912 (1980).
- [14] T. Yanagida, Prog. Theor. Phys. **64**, 1103 (1980).
- [15] F. L. Bezrukov and M. Shaposhnikov, Phys. Lett. **B659**, 703 (2008), 0710.3755.
- [16] M. Shaposhnikov and D. Zenhausern, Phys. Lett. **B671**, 187 (2009), 0809.3395.
- [17] M. Shaposhnikov and D. Zenhausern, Phys. Lett. **B671**, 162 (2009), 0809.3406.
- [18] G. Weidenspointner *et al.*, A&A**450**, 1013 (2006), astro-ph/0601673.
- [19] A. G. Lyne and D. R. Lorimer, Nature **369**, 127 (1994).
- [20] PAMELA, O. Adriani *et al.*, Nature **458**, 607 (2009), 0810.4995.
- [21] H. V. Klapdor-Kleingrothaus, A. Dietz, I. V. Krivosheina, and O. Chkvorets,

- Nucl. Instrum. Meth. **A522**, 371 (2004), hep-ph/0403018.
- [22] DAMA, R. Bernabei *et al.*, Eur. Phys. J. **C56**, 333 (2008), 0804.2741.
- [23] F. Vissani, Phys. Rev. **D57**, 7027 (1998), hep-ph/9709409.
- [24] M. Fukugita and T. Yanagida, Phys. Lett. **B174**, 45 (1986).
- [25] V. A. Kuzmin, V. A. Rubakov, and M. E. Shaposhnikov, Phys. Lett. **B155**, 36 (1985).
- [26] S. Davidson, E. Nardi, and Y. Nir, Phys. Rept. **466**, 105 (2008), 0802.2962.
- [27] A. de Gouvea, Phys. Rev. **D72**, 033005 (2005), hep-ph/0501039.
- [28] S. Dodelson and L. M. Widrow, Phys. Rev. Lett. **72**, 17 (1994), hep-ph/9303287.
- [29] X.-d. Shi and G. M. Fuller, Phys. Rev. Lett. **82**, 2832 (1999), astro-ph/9810076.
- [30] A. D. Dolgov and S. H. Hansen, Astropart. Phys. **16**, 339 (2002), hep-ph/0009083.
- [31] K. Abazajian, G. M. Fuller, and M. Patel, Phys. Rev. D **64**, 023501 (2001), astro-ph/0101524.
- [32] K. Abazajian, G. M. Fuller, and W. H. Tucker, ApJ **562**, 593 (2001), astro-ph/0106002.
- [33] S. Tremaine and J. E. Gunn, Phys. Rev. Lett. **42**, 407 (1979).
- [34] A. Boyarsky, O. Ruchayskiy, and D. Iakubovskiy, JCAP **0903**, 005 (2009), 0808.3902.
- [35] P. B. Pal and L. Wolfenstein, Phys. Rev. **D25**, 766 (1982).
- [36] V. D. Barger, R. J. N. Phillips, and S. Sarkar, Phys. Lett. **B352**, 365 (1995), hep-ph/9503295.
- [37] A. Boyarsky and O. Ruchayskiy, (2008), 0811.2385.
- [38] T. Asaka, M. Shaposhnikov, and A. Kusenko, Phys. Lett. **B638**, 401 (2006), hep-ph/0602150.
- [39] F. L. Bezrukov, A. Magnin, and M. Shaposhnikov, Phys. Lett. **B675**, 88 (2009), 0812.4950.
- [40] F. Bezrukov and M. Shaposhnikov, (2009), 0904.1537.

- [41] A. De Simone, M. P. Hertzberg, and F. Wilczek, *Phys. Lett.* **B678**, 1 (2009), 0812.4946.
- [42] A. O. Barvinsky, A. Y. Kamenshchik, C. Kiefer, A. A. Starobinsky, and C. Steinwachs, (2009), 0904.1698.
- [43] F. Bezrukov, D. Gorbunov, and M. Shaposhnikov, *JCAP* **06**, 029 (2009), 0812.3622.
- [44] WMAP-5, J. Dunkley *et al.*, *Astrophys. J. Suppl.* **180**, 306 (2009), 0803.0586.
- [45] A. D. Sakharov, *Pisma Zh. Eksp. Teor. Fiz.* **5**, 32 (1967).
- [46] K. Kajantie, M. Laine, K. Rummukainen, and M. E. Shaposhnikov, *Phys. Rev. Lett.* **77**, 2887 (1996), hep-ph/9605288.
- [47] F. R. Klinkhamer and N. S. Manton, *Phys. Rev.* **D30**, 2212 (1984).
- [48] M. Shaposhnikov, *JHEP* **08**, 008 (2008), 0804.4542.
- [49] E. K. Akhmedov, V. A. Rubakov, and A. Y. Smirnov, *Phys. Rev. Lett.* **81**, 1359 (1998), hep-ph/9803255.
- [50] A. D. Dolgov, *Sov. J. Nucl. Phys.* **33**, 700 (1981).
- [51] G. Sigl and G. Raffelt, *Nucl. Phys.* **B406**, 423 (1993).
- [52] H. A. Weldon, *Phys. Rev.* **D26**, 2789 (1982).
- [53] M. Laine and M. Shaposhnikov, *JCAP* **6**, 31 (2008), 0804.4543.
- [54] P. D. Serpico and G. G. Raffelt, *Phys. Rev.* **D71**, 127301 (2005), astro-ph/0506162.
- [55] R. Barbieri and A. Dolgov, *Phys. Lett.* **B237**, 440 (1990).
- [56] D. Notzold and G. Raffelt, *Nucl. Phys.* **B307**, 924 (1988).
- [57] T. Asaka, M. Laine, and M. Shaposhnikov, *JHEP* **06**, 053 (2006), hep-ph/0605209.
- [58] T. Asaka, M. Laine, and M. Shaposhnikov, *JHEP* **01**, 091 (2007), hep-ph/0612182.
- [59] K. N. Abazajian and G. M. Fuller, *Phys. Rev.* **D66**, 023526 (2002), astro-ph/0204293.
- [60] K. Abazajian, *Phys. Rev.* **D73**, 063506 (2006), astro-ph/0511630.

- [61] D. Boyanovsky and C. M. Ho, Phys. Rev. **D76**, 085011 (2007), 0705.0703.
- [62] L. Wolfenstein, Phys. Rev. **D17**, 2369 (1978).
- [63] S. P. Mikheev and A. Y. Smirnov, Sov. J. Nucl. Phys. **42**, 913 (1985).
- [64] A. D. Dolgov, S. H. Hansen, G. Raffelt, and D. V. Semikoz, Nucl. Phys. **B580**, 331 (2000), hep-ph/0002223.
- [65] A. D. Dolgov, S. H. Hansen, G. Raffelt, and D. V. Semikoz, Nucl. Phys. **B590**, 562 (2000), hep-ph/0008138.
- [66] D. Gorbunov and M. Shaposhnikov, JHEP **10**, 015 (2007), 0705.1729 [hep-ph].
- [67] A. Boyarsky, J. Lesgourgues, O. Ruchayskiy, and M. Viel, JCAP **0905**, 012 (2009), 0812.0010.
- [68] P. J. E. Peebles, *The large-scale structure of the universe* (Princeton, N.J., Princeton University Press, 1980. 435 p., 1980).
- [69] Y. B. Zel'dovich, A&A**5**, 84 (1970).
- [70] G. S. Bisnovatyi-Kogan, AZh**57**, 899 (1980).
- [71] J. R. Bond, G. Efstathiou, and J. Silk, Phys. Rev. Lett. **45**, 1980 (1980).
- [72] A. G. Doroshkevich, M. I. Khlopov, R. A. Sunyaev, A. S. Szalay, and I. B. Zeldovich, New York Academy Sciences Annals **375**, 32 (1981).
- [73] P. Bode, J. P. Ostriker, and N. Turok, ApJ **556**, 93 (2001), astro-ph/0010389.
- [74] M. Viel, J. Lesgourgues, M. G. Haehnelt, S. Matarrese, and A. Riotto, Phys. Rev. **D71**, 063534 (2005), astro-ph/0501562.
- [75] D. Gorbunov, A. Khmelnitsky, and V. Rubakov, JCAP **0810**, 041 (2008), 0808.3910.
- [76] D. Boyanovsky, H. J. de Vega, and N. G. Sanchez, Phys. Rev. D **77**, 043518 (2008), 0710.5180.
- [77] A. Boyarsky, A. Neronov, O. Ruchayskiy, M. Shaposhnikov, and I. Tkachev, Phys. Rev. Lett.**97**, 261302 (2006), astro-ph/0603660.
- [78] A. Boyarsky, J. Nevalainen, and O. Ruchayskiy, A&A**471**, 51 (2007), astro-ph/0610961.
- [79] A. Boyarsky, A. Neronov, O. Ruchayskiy, and M. Shaposhnikov, Phys. Rev. D **74**, 103506 (2006), astro-ph/0603368.



- [80] A. Boyarsky, D. Iakubovskiy, O. Ruchayskiy, and V. Savchenko, MNRAS **387**, 1361 (2008), 0709.2301.
- [81] A. Boyarsky, A. Neronov, O. Ruchayskiy, and M. Shaposhnikov, MNRAS **370**, 213 (2006), astro-ph/0512509.
- [82] K. N. Abazajian, M. Markevitch, S. M. Koushiappas, and R. C. Hickox, Phys. Rev. D **75**, 063511 (2007), astro-ph/0611144.
- [83] C. R. Watson, J. F. Beacom, H. Yuksel, and T. P. Walker, Phys. Rev. **D74**, 033009 (2006), astro-ph/0605424.
- [84] A. Boyarsky, J. W. den Herder, A. Neronov, and O. Ruchayskiy, Astropart. Phys. **28**, 303 (2007), astro-ph/0612219.
- [85] S. Riemer-Sørensen, S. H. Hansen, and K. Pedersen, ApJ **644**, L33 (2006), astro-ph/0603661.
- [86] A. Boyarsky, O. Ruchayskiy, and M. Markevitch, ApJ **673**, 752 (2008), astro-ph/0611168.
- [87] H. Yuksel, J. F. Beacom, and C. R. Watson, Phys. Rev. Lett. **101**, 121301 (2008), 0706.4084.
- [88] A. Boyarsky, D. Malyshev, A. Neronov, and O. Ruchayskiy, MNRAS **387**, 1345 (2008), 0710.4922.
- [89] M. Loewenstein, A. Kusenko, and P. L. Biermann, (2008), 0812.2710.
- [90] A. Boyarsky, J. Lesgourgues, O. Ruchayskiy, and M. Viel, Phys. Rev. Lett. **102**, 201304 (2009), 0812.3256.
- [91] J. W. den Herder, A. Boyarsky, O. Ruchayskiy, *et al.*, (2009), 0906.1788.
- [92] L. Piro *et al.*, Nuovo Cim. **122B**, 1007 (2007), 0707.4103.
- [93] H. Bi, ApJ **405**, 479 (1993).
- [94] M. Viel, S. Matarrese, H. J. Mo, M. G. Haehnelt, and T. Theuns, Mon. Not. Roy. Astron. Soc. **329**, 848 (2002), astro-ph/0105233.
- [95] M. Zaldarriaga, R. Scoccimarro, and L. Hui, Astrophys. J. **590**, 1 (2003), astro-ph/0111230.
- [96] A. Lewis, A. Challinor, and A. Lasenby, Astrophys. J. **538**, 473 (2000), astro-ph/9911177.
- [97] T. Theuns, A. Leonard, G. Efstathiou, F. R. Pearce, and P. A. Thomas, Mon. Not. Roy. Astron. Soc. **301**, 478 (1998), astro-ph/9805119.

- [98] N. Y. Gnedin and A. J. S. Hamilton, *Mon.Not.Roy.Astron.Soc.* **334**, 107 (2002), astro-ph/0111194.
- [99] P. McDonald *et al.*, *ApJS***163**, 80 (2006), astro-ph/0405013.
- [100] M. Viel, M. G. Haehnelt, and V. Springel, *Mon. Not. Roy. Astron. Soc.* **354**, 684 (2004), astro-ph/0404600.
- [101] M. Viel, M. G. Haehnelt, and V. Springel, *Mon.Not.Roy.Astron.Soc.* **367**, 1655 (2006), astro-ph/0504641.
- [102] M. Viel and M. G. Haehnelt, *Mon. Not. Roy. Astron. Soc.* **365**, 231 (2006), astro-ph/0508177.
- [103] J. A. Regan, M. G. Haehnelt, and M. Viel, *Mon. Not. Roy. Astron. Soc.* **374**, 196 (2007), astro-ph/0606638.
- [104] S. H. Hansen, J. Lesgourgues, S. Pastor, and J. Silk, *MNRAS* **333**, 544 (2002), astro-ph/0106108.
- [105] M. Viel, J. Lesgourgues, M. G. Haehnelt, S. Matarrese, and A. Riotto, *Phys. Rev. Lett.* **97**, 071301 (2006), astro-ph/0605706.
- [106] U. Seljak, A. Makarov, P. McDonald, and H. Trac, *Phys. Rev. Lett.* **97**, 191303 (2006), astro-ph/0602430.
- [107] M. Viel *et al.*, *Phys. Rev. Lett.* **100**, 041304 (2008), 0709.0131.
- [108] A. Klypin, A. V. Kravtsov, O. Valenzuela, and F. Prada, *ApJ* **522**, 82 (1999), astro-ph/9901240.
- [109] S. Ghigna *et al.*, *ApJ* **544**, 616 (2000), astro-ph/9910166.
- [110] B. Moore, T. Quinn, F. Governato, J. Stadel, and G. Lake, *MNRAS* **310**, 1147 (1999), astro-ph/9903164.
- [111] J. Sommer-Larsen and A. Dolgov, *ApJ* **551**, 608 (2001), astro-ph/9912166.
- [112] G. Gilmore *et al.*, *ApJ* **663**, 948 (2007), astro-ph/0703308.
- [113] S. Koposov *et al.*, *ApJ* **663**, 948 (2007), 0706.2687.
- [114] J. T. Kleyana, M. I. Wilkinson, G. Gilmore, and N. W. Evans, *ApJ* **588**, L21 (2003), astro-ph/0304093.
- [115] T. Goerdt, B. Moore, J. I. Read, J. Stadel, and M. Zemp, *MNRAS* **368**, 1073 (2006), astro-ph/0601404.
- [116] F. J. Sánchez-Salcedo, J. Reyes-Iturbide, and X. Hernandez, *MNRAS* **370**,

- 1829 (2006), astro-ph/0601490.
- [117] L. E. Strigari *et al.*, Nature **454**, 1096 (2008), 0808.3772.
- [118] A. V. Kravtsov, A. A. Klypin, J. S. Bullock, and J. R. Primack, ApJ **502**, 48 (1998), astro-ph/9708176.
- [119] A. J. Benson, C. G. Lacey, C. M. Baugh, S. Cole, and C. S. Frenk, MNRAS **333**, 156 (2002), astro-ph/0108217.
- [120] L. E. Strigari *et al.*, ApJ **652**, 306 (2006), astro-ph/0603775.
- [121] J. Klimentowski *et al.*, MNRAS **378**, 353 (2007), astro-ph/0611296.
- [122] L. E. Strigari, M. Kaplinghat, and J. S. Bullock, Phys. Rev. **D75**, 061303 (2007), astro-ph/0606281.
- [123] J. Penarrubia, A. McConnachie, and J. F. Navarro, ApJ **672**, 904 (2008), astro-ph/0701780.
- [124] L. E. Strigari *et al.*, ApJ **669**, 676 (2007), 0704.1817.
- [125] S. E. Kopusov *et al.*, (2009), 0901.2116.
- [126] P. Colin, O. Valenzuela, and V. Avila-Reese, Astrophys. J. **673**, 203 (2008), 0709.4027.
- [127] M. Shaposhnikov, (2007), 0708.3550.
- [128] A. Boyarsky, A. Neronov, O. Ruchayskiy, and M. Shaposhnikov, JETP Letters , 133 (2006), hep-ph/0601098.
- [129] F. Bezrukov, Phys. Rev. **D72**, 071303 (2005), hep-ph/0505247.
- [130] F. Bezrukov and M. Shaposhnikov, Phys. Rev. D **75**, 053005 (2007), hep-ph/0611352.
- [131] M. Shaposhnikov and I. Tkachev, Phys. Lett. **B639**, 414 (2006), hep-ph/0604236.
- [132] A. Anisimov, Y. Bartocci, and F. L. Bezrukov, Phys. Lett. **B671**, 211 (2009), 0809.1097.
- [133] A. Kusenko, Phys. Rev. Lett. **97**, 241301 (2006), hep-ph/0609081.
- [134] K. Petraki and A. Kusenko, Phys. Rev. **D77**, 065014 (2008), 0711.4646.
- [135] K. Petraki, Phys. Rev. D **77**, 105004 (2008), 0801.3470.
- [136] D. Boyanovsky, Phys. Rev. **D78**, 103505 (2008), 0807.0646.

- [137] G. Bertone, W. Buchmuller, L. Covi, and A. Ibarra, *JCAP* **0711**, 003 (2007), 0709.2299.
- [138] K. Kainulainen, J. Maalampi, and J. T. Peltoniemi, *Nucl. Phys.* **B358**, 435 (1991).
- [139] G. Raffelt and G. Sigl, *Astropart. Phys.* **1**, 165 (1993), astro-ph/9209005.
- [140] G. G. Raffelt, *Stars as laboratories for fundamental physics: The astrophysics of neutrinos, axions, and other weakly interacting particles* (University of Chicago Press, Chicago, USA, 1996).
- [141] G. G. Raffelt, *Ann. Rev. Nucl. Part. Sci.* **49**, 163 (1999), hep-ph/9903472.
- [142] X. Shi and G. Sigl, *Phys. Lett.* **B323**, 360 (1994), hep-ph/9312247.
- [143] M. Prakash *et al.*, *Phys. Rept.* **280**, 1 (1997), nucl-th/9603042.
- [144] J. Hidaka and G. M. Fuller, *Phys. Rev. D* **74**, 125015 (2006), astro-ph/0609425.
- [145] J. Hidaka and G. M. Fuller, *Phys. Rev. D* **76**, 083516 (2007), 0706.3886.
- [146] G. M. Fuller, A. Kusenko, and K. Petraki, *Phys. Lett.* **B670**, 281 (2009), 0806.4273.
- [147] A. Kusenko and G. Segre, *Phys. Lett.* **B396**, 197 (1997), hep-ph/9701311.
- [148] M. Barkovich, J. C. D’Olivo, and R. Montemayor, *Phys. Rev.* **D70**, 043005 (2004), hep-ph/0402259.
- [149] G. M. Fuller, A. Kusenko, I. Mocioiu, and S. Pascoli, *Phys. Rev.* **D68**, 103002 (2003), astro-ph/0307267.
- [150] A. Kusenko, B. P. Mandal, and A. Mukherjee, *Phys. Rev.* **D77**, 123009 (2008), 0801.4734.
- [151] A. Kusenko, (2009), 0906.2968.
- [152] P. L. Biermann and A. Kusenko, *Phys. Rev. Lett.* **96**, 091301 (2006), astro-ph/0601004.
- [153] J. Stasielak, P. L. Biermann, and A. Kusenko, *ApJ* **654**, 290 (2007), astro-ph/0606435.
- [154] E. Ripamonti, M. Mapelli, and A. Ferrara, *Mon. Not. Roy. Astron. Soc.* **375**, 1399 (2007), astro-ph/0606483.
- [155] E. Ripamonti, M. Mapelli, and A. Ferrara, *Mon. Not. Roy. Astron. Soc.*

- 374**, 1067 (2007), astro-ph/0606482.
- [156] M. Mapelli, A. Ferrara, and E. Pierpaoli, *Mon. Not. Roy. Astron. Soc.* **369**, 1719 (2006), astro-ph/0603237.
- [157] N. Bilic, R. J. Lindebaum, G. B. Tupper, and R. D. Viollier, *Phys. Lett.* **B515**, 105 (2001), astro-ph/0106209.
- [158] M. C. Richter, G. B. Tupper, and R. D. Viollier, *JCAP* **0612**, 015 (2006), astro-ph/0611552.
- [159] F. Munyaneza and P. L. Biermann, *A&A***458**, L9 (2006), astro-ph/0609388.
- [160] A. Palazzo, D. Cumberbatch, A. Slosar, and J. Silk, *Phys. Rev.* **D76**, 103511 (2007), 0707.1495.